

**An-Najah National University**

**Faculty of Graduate Studies**

**Kinetics, Thermodynamics and Adsorption of  
BTX via Date-Palm Pits Carbonization I  
Aqueous Solution**

**By**

**Rasha Fawzi Khaled Ahmad**

**Supervisors**

**Dr. Shehdeh Jodeh**

**Co-Supervisor**

**Dr. Mohammed Suleiman**

**This Thesis is Submitted in Partial Fulfillment of the Requirements  
for the Degree of Master of Chemistry, Faculty of Graduate Studies,  
An-Najah National University, Nablus, Palestine.**

**2014**

**Kinetics, Thermodynamics and Adsorption of BTX via  
Date-Palm Pits Carbonization in Aqueous Solution**

By

**Rasha Fawzi Khaled Ahmad**

**This Thesis was defended successfully on 23/1/2014 and approved by:**

**Defense Committee Members**

**Signature**

- **Dr. Shehdeh Jodeh / Supervisor**

  
.....

- **Dr. Mohammed Suleiman / Co-Supervisor**

  
.....

- **Dr. Ziad Shakhshir / External Examiner**

  
.....

- **Prof. Dr. Ismail Warad / Internal Examiner**

  
.....

## **Dedication**

My thesis is dedicated to my dear Parents, as well as to my husband, my brothers , my sisters for their support, and everyone helped me to complete it.

With my respect and appreciation.

## **Acknowledgement**

At the beginning I thank Allah who helped me to complete this study. A lot of appreciation to my supervisors Dr. Shehdeh jodeh and Dr. Mohammed Suleiman for their instructions and support which participated in completion this research.

Special thanks to laboratory technician Mr. Omar Nabulsi and Mr. Nafith Dewikat for help and cooperation. Finally, to my family and friends for encouragement and love at all times.

## الإقرار

أنا الموقع أدناه مقدم الرسالة التي تحمل العنوان:

### **Kinetics, Thermodynamics and Adsorption of BTX via Date-Palm Pits Carbonization in Aqueous Solution**

### **الحركية، الديناميكا الحرارية وادمصاص مادة BTX باستخدام بذور البلح المكرينة في محلول مائي**

أقر بأن ما اشتملت عليه هذه الرسالة، إنما هي نتاج جهدي الخاص، باستثناء ما تمت الإشارة إليه  
حيثما ورد، وأن هذه الرسالة ككل، أو أي جزء منها لم يقدم من قبل لنيل أية درجة علمية أو بحث  
علمي أو بحثي لدى أية مؤسسة تعليمية أو بحثية أخرى

### **Declaration**

The work provided in this thesis, unless otherwise referenced, is the  
researcher's own work, and has not been submitted elsewhere for any other  
degree or qualification

**Student's name:**

اسم الطالب:

**Signature:**

التوقيع:

**Date:**

التاريخ:

## Table of Contents

<b>Contents</b>	<b>Page</b>
Dedication	<b>iii</b>
Acknowledgement	<b>iv</b>
Declaration	<b>v</b>
Table of Contents	<b>vi</b>
List of Tables	<b>viii</b>
List of Figures	<b>ix</b>
List of Abbreviations	<b>xii</b>
Abstract	<b>xiii</b>
<b>Chapter One: Introduction</b>	
1.1 Overview	<b>1</b>
1.2 BTX in The Water	<b>1</b>
1.3 Previous Studies	<b>3</b>
1.4 Objectives of this Study	<b>4</b>
<b>Chapter Two: Theoretical Background</b>	
2.1 Date-Palm Pits	<b>5</b>
2.2 Precursors of Activated Carbon	<b>6</b>
2.3 Carbon Activation	<b>6</b>
2.3.1 Physical Activation	<b>7</b>
2.3.2 Chemical Activation	<b>7</b>
2.4 Activating Agents	<b>8</b>
2.4.1 Ferric Chloride	<b>8</b>
2.4.2 Silver Nitrate	<b>8</b>
2.4.3 Copper Sulfate Pentahydrate	<b>9</b>
2.5 Adsorption Isotherm	<b>10</b>
2.5.1 Langmuir equation	<b>10</b>
2.5.2 Freundlich equation	<b>11</b>
2.6 Kinetics Experiments	<b>11</b>
2.6.1 Pseudo First Order Kinetics Model	<b>11</b>
2.6.2 Pseudo Second Order Model	<b>12</b>
2.6.3 Intraparticle Model	<b>12</b>
2.7 Adsorption Thermodynamics	<b>13</b>
<b>Chapter Three: Methodology</b>	
3.1 Materials	<b>14</b>
3.1.1 Precursor	<b>14</b>

3.1.2 Chemicals and Reagents	14
3.2 Preparation of Activated Carbon	15
3.3 Surface Area	16
3.3.1 Iodine Number	16
3.3.2 Brunauer, Emmett and Teller (BET)	18
3.3.3 Scanning Electron Microscope (SEM)	19
3.4 Gas Chromatography (GC-MS)	19
3.6 Adsorption Efficiency	22
3.6.1 Effect of Contact Time	22
3.6.2 Effect of Dosage	23
3.6.3 Effect of Temperature	23
3.6.4 effect of pH	23
3.6.5 effect of concentration	23
<b>Chapter Four: Results and Discussions</b>	
4.1 Carbon Characterization	25
4.2 SEM Analysis of the AC	25
4.4 Adsorption Efficiency of AC	26
4.4.1 Calibration Curve for BTX	26
4.4.2 Effect of Contact Time	27
4.4.3 Effect of Dosage	28
4.4.4 Effect of Temperature	29
4.4.5 Effect of pH	31
4.5 Adsorption Isotherm	32
4.6 Kinetics of Adsorption	36
4.7 Adsorption Thermodynamics	40
<b>Conclusion</b>	<b>42</b>
<b>Suggestions for Future Work</b>	<b>43</b>
<b>References</b>	<b>44</b>
<b>Appendix</b>	<b>56</b>
الملخص	ب

### List of Tables

No.	Table	Page
Table 3.1	The sources of all reagent and chemicals.	<b>14</b>
Table 3.2	SPME conditions.	<b>21</b>
Table 3.3	Gas chromatograph conditions.	<b>22</b>
Table 3.4	Mass spectrometer conditions.	<b>22</b>
Table 4.1	The characteristics of date stones activated carbon.	<b>25</b>
Table 4.2	Langmuir and Freundlich isotherm parameters and correlation coefficient of BTX adsorption onto AC/FeCl <sub>3</sub> .	<b>35</b>
Table 4.3	Pseudo-first-order and pseudo-second-order kinetic model parameters for BTX adsorption by AC/ FeCl <sub>3</sub> .	<b>38</b>
Table 4.4	The values of $q_t$ and $t^{0.5}$ for intra-particle diffusion kinetic model.	<b>39</b>
Table 4.5	Intra-particle diffusion kinetic model parameters for BTX adsorption by AC/ FeCl <sub>3</sub> .	<b>39</b>
Table 4.6	The values of the thermodynamic of adsorption at various temperatures and various adsorbents.	<b>41</b>



## List of Figures

No.	Figure	Page
Figure3.1	The flow diagram for activation process.	<b>16</b>
Figure 3.2	Standard calibration curve for iodine number.	<b>18</b>
Figure 3.3	Gas Chromatography with Mass Spectrometer.	<b>20</b>
Figure 3.4	SPME device.	<b>21</b>
Figure 4.1	SEM micrographs of AC/FeCl <sub>3</sub>	<b>26</b>
Figure 4.2	Calibration curve for BTX standard solutions at 25°C.	<b>27</b>
Figure 4.3	Effect of contact time on the adsorption of BTX by AC/FeCl <sub>3</sub> at initial concentration 50 ppm, pH: 4, temperature: 25°C and 0.25g of AC.	<b>28</b>
Figure 4.4	Effect of AC dosage on the adsorption of BTX by AC/FeCl <sub>3</sub> at initial concentration 50 ppm, pH: 4 and temperature: 25°C for 30 min.	<b>29</b>
Figure 4.5	Effect of temperature on BTX removal by AC/FeCl <sub>3</sub> at initial conc:50 ppm, pH: 4 and temperature: 25°C for 30 min.	<b>29</b>
Figure 4.6	Effect of pH on the adsorption of BTX by AC/FeCl <sub>3</sub> at initial concentration 50 ppm, 0.25g of AC and temperature: 25°C for 30 min.	<b>31</b>
Figure 4.7.a	Langmuir plot for benzene adsorption onto AC/FeCl <sub>3</sub> at temperature: 25°C, pH: 4 and solid/liquid ratio 0.25 g/50 mL.	<b>32</b>
Figure 4.7.b	Langmuir plot for toluene adsorption onto AC/FeCl <sub>3</sub> at temperature: 25°C, pH: 4 and solid/liquid ratio 0.25 g/50 mL.	<b>33</b>
Figure 4.7.c	Langmuir plot for xylene adsorption onto AC/FeCl <sub>3</sub> at temperature: 25°C, pH: 4 and solid/liquid ratio 0.25 g/50 mL	<b>33</b>
Figure 4.8.a	Freundlich plot for benzene adsorption onto AC/FeCl <sub>3</sub> at temperature: 25°C, pH: 4 and	<b>34</b>

	solid/liquid ratio 0.25 g/50 mL).	
Figure 4.8.b	Freundlich plot for toluene adsorption onto AC/FeCl <sub>3</sub> at temperature: 25°C, pH: 4 and solid/liquid ratio 0.25 g/50 mL).	<b>34</b>
Figure 4.8.c	Freundlich plot for xylene adsorption onto AC/FeCl <sub>3</sub> at temperature: 25°C, pH: 4 and solid/liquid ratio 0.25 g/50 mL).	<b>35</b>
Figure 4.9	Kinetics of BTX removal according to the pseudo-first-order model by AC/FeCl <sub>3</sub> at temperature: 25°C, pH: 4 and solid/liquid ratio 0.25 g/50 mL).	<b>37</b>
Figure 4.10	Kinetics of BTX removal according to the pseudo-second-order model by AC/FeCl <sub>3</sub> at temperature: 25°C, pH: 4 and solid/liquid ratio 0.25 g/50 mL).	<b>38</b>
Figure 4.11	Kinetics of BTX removal according to the intra-particle diffusion model by AC/FeCl <sub>3</sub> at temperature: 25°C, pH: 4 and solid/liquid ratio 0.25 g/50 mL).	<b>39</b>
Figure 4.12	Plot of ln K <sub>d</sub> versus 1/T for BTX adsorption on AC/ FeCl <sub>3</sub> .	<b>40</b>

### List of Abbreviation

<b>Symbol</b>	<b>Abbreviation</b>
<b>A</b>	Intra-particle diffusion constant gives an idea about the thickness of the boundary layer.
<b>AC</b>	Activated carbon.
<b>B</b>	Langmuir constant related to the rate of adsorption.
<b>C<sub>o</sub></b>	Initial liquid-phase concentration of adsorbate.
<b>C<sub>Ae</sub></b>	The amount adsorbed on solid at equilibrium.
<b>C<sub>e</sub></b>	Equilibrium liquid-phase concentration of the adsorbate.
<b>GC</b>	Gas chromatography
<b>IN</b>	Iodine number for surface area calculation.
<b>K<sub>d</sub></b>	The distribution coefficient.
<b>K<sub>F</sub></b>	Freundlich constant represents the quantity of adsorbate onto activated carbon per a unit equilibrium concentration.
<b>k<sub>i</sub></b>	The intraparticle diffusion constant .
<b>k<sub>1</sub></b>	The equilibrium rate constant of pseudo-first order kinetic model.
<b>k<sub>2</sub></b>	The equilibrium rate constant of pseudo-second order kinetic model.
<b>M</b>	The mass of dry adsorbent used.
<b>N</b>	The normality of sodium thiosulfate solution.
<b>N</b>	Freundlich constant.

<b>PR%</b>	The amount of removal percentage of BTX by AC.
<b>Q<sub>o</sub></b>	Langmuir constants related to adsorption capacity.
<b>Q<sub>e</sub></b>	Amount of adsorbate per unit mass of adsorbent at equilibrium.
<b>q<sub>t</sub></b>	Amount of adsorbate per unit mass of adsorbent at time t.
<b>R</b>	The universal gas constant (8.314 J/mol K).
<b>R<sup>2</sup></b>	Correlation coefficient.
<b>SEM</b>	Scanning Electron Microscopy.
<b>SPME</b>	Solid-Phase Micro Extraction
<b>T</b>	The absolute solution temperature.
<b>V</b>	Volume of the solution.
<b>V<sub>b</sub></b>	Volume of sodium thiosulfate solution required for blank titration in iodine number calculation.
<b>V<sub>s</sub></b>	Volume of sodium thiosulfate solution required for sample titration iodine number calculation.
<b>W<sub>c</sub></b>	The mass of activated carbon used.
<b>ΔH°</b>	Standard enthalpy.
<b>ΔS°</b>	Standard entropy.
<b>ΔG°</b>	Standard free energy.

**Kinetics, Thermodynamics and Adsorption of BTX in Aqueous  
Solution via Date-Palm Pits Carbonization**

**By**

**Rasha Ahmad**

**Supervisor**

**Shehdeh Jodeh**

**Co-Supervisor**

**Mohammed Suleiman**

**Abstract**

Activated carbon has been the most widely used as adsorbent, which is a versatile adsorbent due to its large area, porous structure, high adsorption capacity and variable surface chemical composition. Benzene, toluene and xylene (BTX) compounds are toxic organic compounds that appear in underground water resources as results of leakage from underground fuel tanks and also improper waste discharge of oil and petrochemical industries.

In this work, Palm date pits (Majhool) were used as the precursor in the preparation of activated carbon. The date pits were first washed with water to get rid of impurities, dried at 110 °C for 24 h, crushed, then it was mixed with FeCl<sub>3</sub>, AgNO<sub>3</sub> and CuSO<sub>4</sub>·5H<sub>2</sub>O solution (as activating

agent) at an impregnation ratio of 1:2 for 24 h at room temperature. The impregnated samples were next dried at 110 °C. A stainless steel reactor was used for the carbonization of dried impregnated sample. The reactor was placed in a tube furnace and heated to reach an activation temperature (700 °C).

Adsorption of BTX compounds from water by using activated carbon produced from date palm pits activated by FeCl<sub>3</sub> was investigated in terms of contact time, adsorbent dose, temperature, pH and BTX concentration. Results indicated that the adsorption effectiveness was increased with increasing the pH, dose amount and the contact time. On the other hand, the adsorption efficiency was found to increase with decreasing the temperature.

The equilibrium adsorption isotherm was explained using Langmuir and Freundlich models. BTX adsorption was better represented by Langmuir model. The kinetic of adsorption was studied using pseudo-first order, pseudo-second order and intraparticle diffusion. It was found that the adsorption followed pseudo-second order. Adsorption thermodynamic parameters for BTX adsorption such as standard

xvi

enthalpy  $\Delta H^\circ$ , standard entropy  $\Delta S^\circ$  and standard free energy  $\Delta G^\circ$  were calculated.

The shape, size and surface area of the samples were determined using SEM, iodine number and BET. The effect of activating agent on the adsorption efficiency of BTX was also studied.

# Chapter One

## Introduction

### 1.1 Overview

Water is one of the most valuable resources on planet earth, it is the lifeline of almost all living thing on earth. Although this fact is widely recognized, pollution of water resources is a common occurrence. During the last few decades, the rise of world population as well as industrial revolution has caused serious environmental pollution [1]. And that has attracted a great deal of scientific, political, and media attention. Several dramatic accidents such as oil spills happened in the 1970s and latest in 2010 (British petroleum oil spillage in the Gulf of Mexico). Water pollution is the contamination of water bodies (e.g. lakes, rivers, oceans, aquifers and groundwater). Water pollution occurs when pollutants are discharged directly or indirectly into water bodies without adequate treatment to remove harmful compounds [2].

Water pollution caused by inorganic and organic contaminants has steadily increased in parallel with world population, industrialization, and urbanization especially in developing countries [3].

### 1.2 BTX in the Water

Benzene, toluene and xylene (BTX) isomers are monocyclic aromatic hydrocarbons, which have a moderate solubility in water (benzene: 1600



mg/L; toluene: 500 mg/L and xylenes: 160 mg/L). These compounds are the major water-soluble constituents of petroleum derivatives (gasoline) [4]. In USA, it was found that the maximum level of benzene, toluene and xylene in drinking water to be 0.005, 1 and 10 mg/L respectively [5]. While in Palestine, there is no study in this regard yet.

BTX compounds are toxic organic compounds that appear in underground water resources as results of leakage from underground fuel tanks, cracked pipelines, and also improper waste discharge of oil and petrochemical industries [5, 6, 7].

These pollutants have been found to cause many serious health side effects to humans (e.g. skin and sensory irritation, central nervous system depression, respiratory problems, leukemia, cancer, as well as disturbance of kidney, liver and blood systems) and therefore their removal from groundwater and surface water is essential [8].

Several processes have been examined for removal of BTX compounds from aqueous environment including oxidation, bioremediation and adsorption. Activated carbon has been the most widely used adsorbent, which is a versatile adsorbent due to its large area, polymodal porous structure, high adsorption capacity and variable surface chemical composition [9].

In this study the date pits will be collected and carbonized to increase the adsorption capacity. Then the carbonized date will be used for treating

wastewater by removing BTX. Different physical properties like isotherm, effect of pH and temperatures will be studied.

### **1.3 Previous Studies**

The first known use of activated carbon dates back to the ancient Egyptians who utilized its adsorbent properties for purifying oils and medicinal purposes [10].

Date palm wastes have been used by different researchers as adsorbents for removing of water pollutants such as heavy metals and dyes.

Al-Ghouti et al. [11] investigated the adsorption mechanism of removing heavy metal ions ( $\text{Cu}^{2+}$  and  $\text{Cd}^{2+}$ ) from aqueous solution using date pits as adsorbent. While, El-Hendawy [12] studied the adsorption of  $\text{Pb}^{2+}$  and  $\text{Cd}^{2+}$  ions onto date pits activated carbons.

Ashour [13] studied the kinetics and equilibrium adsorption of methylene blue and remazol dyes onto the steam processed activated carbons developed from date pits.

In the other hand, activated carbon has been used for removal of phenolic and pesticides pollutants. For example, the potential of raw date stone powder for phenol adsorption from aqueous solution was studied by Okasha and Ibrahim [14].

Danish et al [15] reported the kinetics for the removal of paraquat dichloride from aqueous solution by calcium oxide activated date stone carbon.

Adsorption of herbicide (Pendimethalin) onto activated carbons developed from date pits were studied by Ashour [16]. Also, it have been used for removal of miscellaneous pollutants, such as, El-Naas et al [17] carried out experiments to evaluate the batch adsorption of chemical oxygen demand (COD).

#### **1.4 Objectives of this Study**

Due to the increasing sources of pollution in the world, the impact of water pollution on human health is getting more crucial. This study is focused on studying the impact of water pollution by BTX. The main objectives of this study can be summarized by the following points:

- Finding a good method for carbonization of date.
- Using activated carbon for removing BTX from water.
- Studying the effect of activating agent.
- Studying the adsorption kinetic of contaminant on carbonization of date.
- Studying the adsorption isotherm and thermodynamics of contaminant on carbonization of date.
- Determining the effect of temperature, adsorbent dose, pH, time and concentration on adsorption of contaminant.

## Chapter Two

### Theoretical Background

This chapter includes an explanation about the used materials and Equations.

#### 2.1 Date-Palm Pits

The date palm is one of the oldest fruit trees in the world and is mentioned in the Qur'an and Bible. The number of the date palms is about 100 million worldwide, of which 62 million palms can be found in the Arab world [18, 19]. The place of origin of the date palm is uncertain. Some claim that the date palm first originated in Babel, Iraq, while others believe that it originated in Dairen or Hofuf, Saudi Arabia [20].

Date stones are suitable for use in animal feed and their oil is used in soap and cosmetics. They can also be processed chemically as a source of oxalic acid. Date seeds are also ground and used in the manner of coffee beans, or as an additive to coffee [20].

Date palm consists of three main components: cellulose, hemicellulose, and lignin in the range of 40–50%, 20–35%, and 15–35%, respectively, besides these other minor constituents are oil and protein [21]. Cellulose and hemicellulose consists of glucose units but hemicelluloses consists of the lower number of saccharide units. Both have average percent elemental compositions of 44.4 wt. % carbon, 49.4 wt. %

oxygen, and 6.2 wt. % hydrogen. Lignin has more complex chemical constituents.

It has a three-dimensional polymer of phenylpropane units linked together by C–O–C or C–C bonds. This makes its elemental composition to be higher in carbon percentage (62 wt. %) and lower in oxygen percentage (32 wt. %) [22].

## **2.2 Precursors of Activated Carbon**

Precursors of activated carbons are organic materials with high carbon content [23]. The most widely used carbonaceous materials for the industrial production of activated carbons are coal, wood and coconut shell [24, 25].

Activated carbon can be produced from any natural or synthetic carbonaceous precursor which is largely dependent on its availability, cost and purity. Due to environmental considerations, agricultural wastes are considered to be a very important precursor because they are cheap, renewable, safe, available at large quantities and easily accessible sources; in addition they have high carbon and low ash content [26, 27].

## **2.3 Carbon Activation**

Carbon treatment has been used since Roman times to purify different materials [28]. The production of activated carbon from agricultural waste materials has been the purpose of several studies, among which we can

mention activated carbons prepared from nut shells [29], rice husks [30], peach stones [31], cane sugar [32], fruit rind [33] and peanut husks [34]. Activated carbon can be produced by physical or chemical activation.

### **2.3.1 Physical Activation**

The physical activation process involves two steps: the first one is the carbonization of the carbonaceous precursor [35] at elevated temperatures (500-1000°C) under inert atmosphere in order to eliminate oxygen and hydrogen elements as far as possible [36].

The second stage involves mild oxidation (gasification) with steam (air, carbon dioxide). This can be done at the same temperature for pyrolysis or at a higher temperature (800-1000°C) [37,38].

### **2.3.2 Chemical Activation**

Chemical activation involves impregnation of the precursor with chemical activating agents (mostly dehydrating agents such as  $\text{ZnCl}_2$ ,  $\text{KOH}$ ,  $\text{FeCl}_3$ ) followed by pyrolysis at relatively low temperature than physical activation temperature. The chemical activating agent incorporated into the bulk of the precursor particles, which make way for a chemical reaction between the surface chemical constituents of precursor and activating agents. These chemical reactions form many stable and volatile complexes. The volatile complexes evaporate during pyrolysis (such as oxygen and hydrogen) and the stable complexes remains (carbon) to give pores shape [9].

## **2.4 Activating Agents**

### **2.4.1 Ferric Chloride**

Ferric chloride is a chemical compound, with the formula  $\text{FeCl}_3$ . The color of its crystals depends on the viewing angle (the crystals appear dark green by reflected light, but by transmitted light they appear purple-red) [39].

Although the iron chloride salt has similar characteristics to zinc chloride in aqueous solution, the ferric cation is smaller than the zinc cation, and this opens up the possibility of producing activated carbon with smaller pores sizes. On the other hand, the zinc cation presented in aqueous solution is a well-known pollutant. Moreover, the ferric salt has a low cost in comparison with the zinc salt [40].

The use of ferric chloride is not completely new. Oliveira et al [41] and Rufford et al [42] used it to prepare activated carbons from coffee husks and waste coffee grounds, respectively.

### **2.4.2 Silver Nitrate**

Silver nitrate is an inorganic compound, colorless crystalline material and high solubility in water with chemical formula  $\text{AgNO}_3$ . This compound is a versatile precursor to many other silver compounds [43]. It is used in chemical analysis for silver plating, in inks, hair dyes, silver

mirrors and for detection of reducing agents and the cations of various acids that form insoluble silver salts, as well as in medicine for treatment of eye infections.

Ingestion of silver nitrate causes violent abdominal pains, vomiting, and diarrhea, with the development of gastroenteritis. Treatment includes oral administration of common salt solutions, milk (or white of egg and water), and soap in water to protect the mucous membranes of the esophagus and stomach [44].

### **2.4.3 Copper Sulfate Pentahydrate**

Copper (II) sulfate is an inorganic chemical compound, odorless and appears blue in color with  $\text{CuSO}_4$  chemical formula [45].

Copper Sulfate pentahydrate is a hazardous chemical and should be handled with safety spectacles and rubber gloves. This compound is acidic and irritates eyes and the respiratory tract upon contact. It is absorbed through the skin, causing severe itching and eczema. If swallowed, it causes nausea, vomiting, headaches and burning chest pains [46].

Copper Sulfate is used as an electrolyte in copper refining and electroplating and mining. The building uses copper sulphate in combination with other chemicals as a wood preservative. In agriculture, it is widely used as a micronutrient in animal feeds and fertilizers. Its fungicidal properties are utilized in the growing of grapes and fruit trees [47].



The used activating agents were chosen based on different properties and the sizes of the particles.  $\text{FeCl}_3$  is a well known activating agents and to the best of our knowledge  $\text{AgNO}_3$  and  $\text{CuSO}_4 \cdot 5\text{H}_2\text{O}$  will be used for the first time as activating agents in this study.

## 2.5 Adsorption Isotherm

Adsorption isotherm is the amount of adsorbate on the adsorbent as a function of its pressure (if gas) or concentration (if liquid) at constant temperature [53].

### 2.5.1 Langmuir Equation

This Equation used for the molecules that are in contact with a solid surface at a fixed temperature. The Langmuir Isotherm developed by Irving Langmuir between 1909-1916. It assumes a monolayer adsorption onto a uniform adsorbent surface with energetically identical sorption sites [56]. The linear form of Langmuir isotherm Equation is described by the following Equation:

$$\frac{C_e}{q_e} = \frac{1}{b q_0} + \frac{C_e}{q_0} \quad (2.1)$$

Where  $C_e$  is the equilibrium concentration of the adsorbate (mg/L),  $q_e$  is the amount of adsorbate per unit mass of adsorbent (mg/g),  $q_0$  and  $b$  are Langmuir constants related to adsorption capacity and rate of adsorption, respectively.

### 2.5.2 Freundlich Equation

In 1909, Freundlich gave an empirical expression representing a relationship between the concentrations of a solute on the surface of an adsorbent, to the concentration of the solute in the liquid.

It describes equilibrium on heterogeneous surfaces and hence does not assume mono layer capacity [56]. The logarithmic form of the Freundlich isotherm is given by the following Equation:

$$\log q_e = \log K_f + \left(\frac{1}{n}\right) \log C_e \quad (2.2)$$

Where  $C_e$  is the equilibrium concentration of the adsorbate (mg/L),  $q_e$  is the amount of adsorbate per unit mass of adsorbent (mg/g),  $K_f$  and  $n$  are Freundlich constants.

## 2.6 Kinetics Experiments

The process of removal BTX can be explained by using several kinetics models. In this study we used the first, second pseudo order and intraparticle models [57].

### 2.6.1 Pseudo-First Order Kinetics Model

Is a second order reaction, in which one of the reactants is present in such great amounts that its effect is not seen and the reaction thus behaves as first order.

The simple form of first order model, is shown in Eq.(2.3) [58].

$$\ln(q_e - q_t) = \ln q_e - k_1 t \quad (2.3)$$

Where  $k_1$  is the rate constant,  $q_e$  is the equilibrium concentration (mg/g);  $q_t$  (mg/g) is the amount of adsorbed at any time  $t$  (min).

### 2.6.2 Pseudo -Second Order Model

The general form of the model is given in Eq. (2.4) [59].

$$\frac{t}{q_t} = \frac{1}{k_2 q_e^2} + \frac{1}{q_e} t \quad (2.4)$$

In which,  $k_2$  is the equilibrium rate constant (g/mg.min) of pseudo-second order.  $q_e$  is the amount of adsorption sorbed at equilibrium (mg. g<sup>-1</sup>),  $q_t$  is the amount of adsorbate sorbed at  $t$  (min). The straight line plots of  $(t/q_t)$  vs  $t$  have been tested to obtain rate parameters [60].

### 2.6.3 Intraparticle Model

Intraparticle diffusion model can be expressedby Weber and Morris [62], as the Eq.( 2.5)

$$q_t = k_i t^{0.5} + A \quad (2.5)$$

Where  $k_i$  is the intraparticle diffusion constant and  $q_t(\text{mg/g})$  is the amounts of adsorbate per unit mass of adsorbent at time  $t$  (min) the intercept  $A$  reflects the effects of the boundary layer thickness.

## 2.7 Adsorption Thermodynamics

Thermodynamic considerations of the adsorption process of BTX on date stones are necessary to conclude whether the process is favorable or not.

This behavior was evaluated by the thermodynamic parameters including the change in free energy ( $\Delta G^\circ$ ), enthalpy ( $\Delta H^\circ$ ), and entropy ( $\Delta S^\circ$ ).

$$\ln k_d = \frac{\Delta S^\circ}{R} - \frac{\Delta H^\circ}{R} \frac{1}{T} \quad (2.6)$$

Where  $T$  (K) is the absolute solution temperature,  $R$  (8.314 J/mol K) is the universal gas constant and  $K_d$  is the distribution coefficient which can be calculated as:

$$K_d = C_{Ae}/C_e \quad (2.7)$$

Where  $C_{Ae}$  (mg/L) is the amount adsorbed on solid at equilibrium and  $C_e$  (mg/L) is the equilibrium concentration.  $\Delta G^\circ$  can be calculated as below:

$$\Delta G^\circ = -RT \ln K_d \quad (2.8)$$

## Chapter Three

### Methodology

#### 3.1 Materials

##### 3.1.1 Precursor

Palm date pits (Majhool) were used as the precursor in the preparation of activated carbon. The date pits were first washed with water to get rid of impurities, dried at 110 °C for 24 h, crushed using stainless steel mill, and sieved.

##### 3.1.2 Chemicals and Reagent

All chemicals such as hydrochloric acid, sodium thiosulfate, iodine and sodium hydroxide were used for analytical grades. FeCl<sub>3</sub>, AgNO<sub>3</sub> and CuSO<sub>4</sub>·5H<sub>2</sub>O are used as chemical reagents for activation of date pits. Benzene, toluene and xylene were used as adsorbate. The sources of all reagent and chemicals which was used are summarized in Table 3.1.

**Table 3.1:** The sources of all reagent and chemicals.

Name	Company	Catalog
Benzene	MercK	1782
Xylene	J.T.Baker	9493-03
AgNO <sub>3</sub>	Riedel	31630
Toluene	Frutarom	2355540500024
CuSO <sub>4</sub> ·5H <sub>2</sub> O	Frutarom	23555115500
HCl	MercK	1.00319
FeCl <sub>3</sub>	Riedel	12321

### 3.2 Preparation of Activated Carbon

Where, 50 g of crushed stones was well mixed with 500 ml  $\text{FeCl}_3$ ,  $\text{AgNO}_3$  or  $\text{CuSO}_4 \cdot 5\text{H}_2\text{O}$  solution at an impregnation ratio of 2 (weight of activating agent to weight of dried stone) for 24 h at room temperature. The impregnated samples were next dried at  $110^\circ\text{C}$  until completely dried and stored in a desiccator. A stainless steel reactor was used for the carbonization of dried impregnated sample. This reactor was closed at one end and the other end had a removable cover with two holes, one for inter the nitrogen and the other for escape of the pyrolysis gases. The reactor was placed in a tube furnace and heated to reach an activation temperature ( $700^\circ\text{C}$ ) for 30 min; until no gas rising. At the end of activation time the carbonized sample was withdrawn from the furnace and allowed to cool. For removal of residual activated agent, the sample was soaked with 0.1M HCl solution such that the liquid to solid ratio is 10ml/g. The mixture was left overnight at room temperature and then it was filtered and was washed with distilled water until the pH of filtrate reached 6.5-7; to wash HCl and to make it neutral [62].

After that, the sample was dried at  $110^\circ\text{C}$  for 24 h and subsequently was weighed to determine the yield of the product. Finally, it was stored in closed bottles. The flow diagram for activation process is summarized in Fig. 3.1.

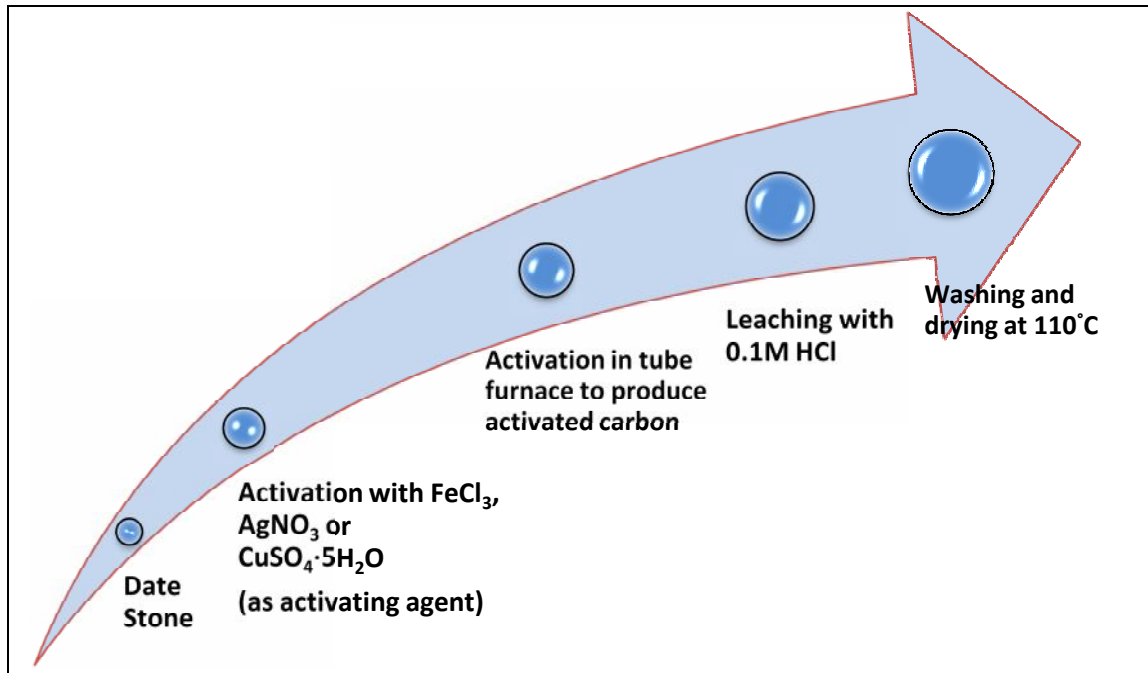


**Figure 3.1:** The flow diagram for activation process.

The yield of the activated carbon was estimated from the following Equation:

$$\text{yield of activated carbon (\%)} = \frac{\text{weight of activated carbon}}{\text{weight of waste date stones}} \times 100 \% \quad (3.1)$$

### 3.3 Surface Area

The surface area is the sum of all areas of the activated carbon particles used. The surface areas of the prepared activated carbons were found by estimated iodine number and Brunauer, Emmett and Teller (BET).

#### 3.3.1 Iodine Number

Basically, iodine number is a measure of the micropore content of activated carbon (0 to 20 Å) by adsorption of iodine from solution [64].

It was found by titration 10 mL of 0.1N iodine solution with 0.1N sodium thiosulfate solution in the presence of starch solution as indicator, until it becomes colorless. The reading of burette is corresponding to  $V_b$ . Then 0.05g of activated carbon was added to 15 mL of 0.1N iodine solution, the mixture was shaken for 5min and then was filtered. 10 mL of the filtrate was titrated with 0.1N standard sodium thiosulfate solution in the presence of starch solution as indicator. The burette reading is corresponding to  $V_s$ . The following Equation was used to calculate the iodine number.

$$IN = \frac{(V_b - V_s) \cdot N \cdot (126.9) \cdot (15/10)}{W_c} \quad (3.2)$$

Where IN is iodine number (mg/g),  $V_b$  and  $V_s$  are volumes of sodium thiosulfate solution required for blank and sample titrations (mL), respectively, N is the normality of sodium thiosulfate solution (mole/L), 126.9 g is atomic weight of iodine, and  $W_c$  is the mass (g) of activated carbon.



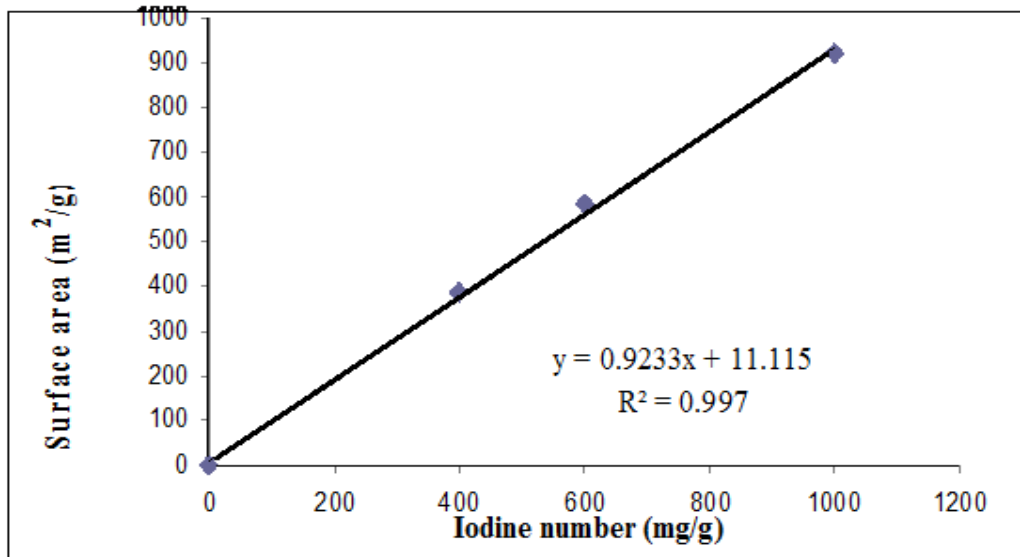


**Figure 3.2:** standard calibration curve for iodine number [65].

### 3.3.2 Brunauer, Emmett and Teller (BET)

The BET theory was developed by Stephen Brunauer, P.H. Emmet and Edward Teller in 1938.

This theory aims to explain the physical adsorption of gas molecules on a solid surface and serves as the basis for an important analysis technique for the measurement of the specific surface area and pore size distribution for a wide variety of samples, including powders and bulk solids [65]. The BET machine has a multitude of applications in industries worldwide. Some applicable industries include Rubber, Chemical, Ceramic, Paper, Battery Separator, Fuel Cells and Pharmaceuticals. It is the most advanced, accurate, easy to use and reproducible parameters in the world [66].

### **3.3.3 Scanning Electron Microscopy (SEM)**

Is a type of electron microscope that produces images of a sample by scanning it with a focused beam of electrons. The electrons interact with atoms in the sample, producing various signals that can be detected and that contain information about the sample's surface topography and composition [67].

The SEM image was performed in the University of Jordan/ Faculty of Science. The SEM device has a high-brightness, high-current, high-resolution imaging, a SEM equipped with a high resolution Schottky Field Emission source, provides clear, sharp and noise-free imaging. The system's excellent lateral resolution enables easy detection of low-Z elements at low beam energies, adding value and flexibility to the Inspect F50.

### **3.4 Gas Chromatography (GC-MS)**

Gas Chromatography (Figure3.3) is a method that combines the features of gas chromatography and mass spectrometry for chemical identification of volatile and semi-volatile organic compounds in mixtures, drug detection, environmental analysis and explosives investigation. Additionally, it can identify trace elements in materials that were previously thought go undetected by other technologies [48].

Solid-Phase Micro Extraction (SPME) (Figure 3.4) is a solvent-free sampling and sample preparation technique, which combines sampling, pre-concentration and the direct transfer of the analytes into a GC or HPLC [49].

In SPME technique, analytes of interest are allowed to adsorb onto a small microfiber made of a fused silica coated with a thin-film of stationary phase. Analytes either in the air or in an aqueous sample come into equilibrium with the fiber according to their affinity for the solid phase [50]. The microfiber, which is incorporated into a gas chromatography (GC) syringe, is directly injected into the GC. Because the SPME fiber is heated at the GC injection port to allow the analytes to be desorbed from the fiber, the injection is directly to the GC without solvent [41].



**Figure 3.3:** Gas Chromatography with Mass Spectrometer (GC-MS).

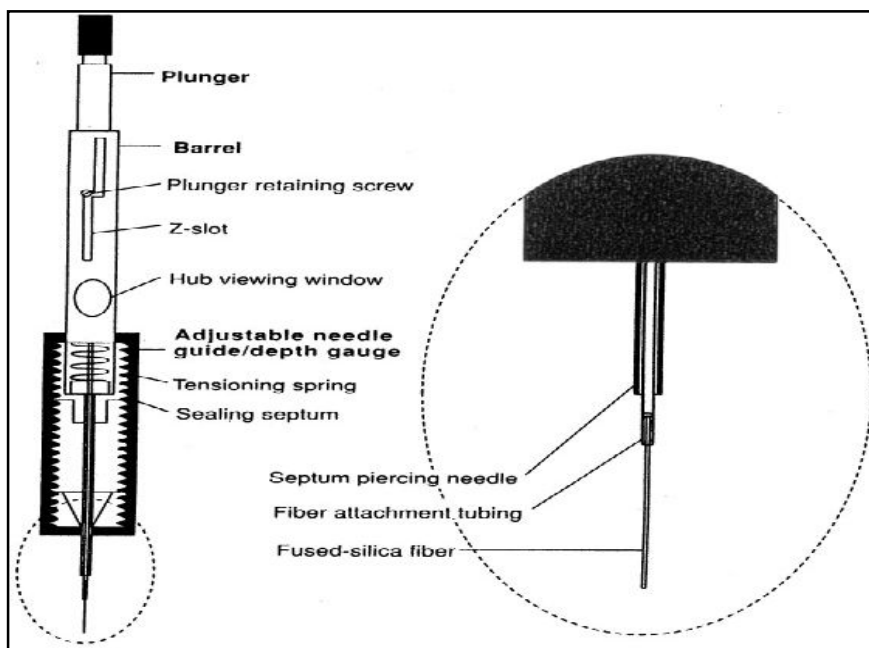


**Figure 3.4:** SPME device [taken from Ref.52].

In this work, the GC-MS was used to determine the effect of contact time, dosage, temperature and pH on the adsorption by finding the peak area<sup>1</sup> at equilibrium.

The analysis of BTX in water samples was conducted by SPME, GC/MS using the Clarus SQ 8S Mass Spectrometer. The DB-5 column (60 m × 0.53 mm × 0.5 μm) was used. The experimental conditions are presented in Tables 3.2- 3.4.

**Table 3.2:** SPME Conditions.

<b>Sample Temperature</b>	80 °C
<b>Needle Temperature</b>	110 °C
<b>Transfer Line Temperature</b>	120 °C
<b>SPME Low/ SPME High</b>	35 °C to 260 °C

<sup>1</sup>The peak area for the calibration curve are shown in appendix A, section A.1.

<b>Equilibration Time</b>	8 min
---------------------------	-------

**Table 3.3:** Gas Chromatograph Conditions.

<b>GC/MS</b>	Clarus SQ 8S
<b>Column</b>	DB-5 ( 60 m x 0.53 mm x 0.5 $\mu$ m )
<b>Oven</b>	40 °C for 0.5 min, then 35 °C/ min to 185 °C
<b>Injector (PSS)</b>	Temp Programmable Split/Splitless at 180 °C
<b>Carrier Program (He)</b>	1 mL/ min for 0.4 min, then 0.7 mL/ min

**Table 3.4:** Mass Spectrometer Conditions.

<b>Ionization Mode</b>	Electron Impact
<b>Acquisition</b>	Full Scan
<b>Filament Delay</b>	1.5 min
<b>Scan Speed</b>	0.15 sec
<b>Interscan Delay</b>	0.04 sec
<b>Run Time</b>	4 min
<b>Ion Source Temperature</b>	200 °C
<b>Transfer Line Temperature</b>	200 °C

### 3.6 Adsorption Efficiency

Several factors could be affected on the adsorption efficiency by using activated carbon produced from date stone with  $\text{FeCl}_3$  as activating agent, which have been studied in this work as shown below.

#### 3.6.1 Effect of contact time

To study the effect of time, 1g of activated carbon was added to 50 mL BTX solution (50 ppm) by volume at pH 4 and 25°C. These steps were repeated for different time intervals.

### 3.6.2 Effect of Dosage

Different weights was added to 50 mL (50 ppm) BTX solutions at 25°C and pH 4 for 30 min, the effect of dosage was determined.

### 3.6.3 Effect of Temperature

This effect was studied by adding 0.25 g of activated carbon to 50 mL (50 ppm) BTX solutions at pH 4 for 30 min at different temperatures.

### 3.6.4 Effect of pH

This effect was studied using 0.25 g of activated carbon which were added to 50 mL (50 ppm) BTX solutions for 30 min at 25°C and different pH.

### 3.6.5 Effect of concentration

To study the effect of concentration; 0.25 g of activated carbon was added to 50 mL of 10, 20, 30 and 40 ppm solutions at pH 4 and 25°C for 30 min. The initial and final concentrations of BTX were measured.

The amount of adsorption at equilibrium,  $q_e$ , was calculated by using the following Equation:

$$q_e (\text{mg} / \text{g}) = \frac{(C_o - C_e) \cdot v}{m} \quad (3.3)$$

Where  $C_o$  and  $C_e$  (mg/L) are the liquid-phase concentration of drugs initially and at equilibrium, respectively.  $v$  is the volume of the solution (L) and  $m$  is the mass of dry adsorbent used (g). The data were fitted to

Langmuir and Freundlich isotherms to evaluate the adsorption parameters.

The amount of removal percentage of BTX by AC was calculated according to the following expression:

$$\text{PR (\%)} = \frac{C_o - C_e}{C_o} \times 100 \% \quad (3.4)$$

Where PR is the removal percentage (%),  $C_o$  and  $C_e$  are the initial and equilibrium concentration of BTX solution (mg/L), respectively.

## Chapter Four

### Results and Discussions

#### 4.1 Carbon Characterization

The characteristics of date stones activated carbon were studied and calculated by the Equations 3.1, 3.2 and Figure 3.2. The data are summarized in Table 4.1. The results showed higher surface area which means that the use of date stones as activated carbon for removal of BTX from aqueous solutions was successful. On the other hand, the high iodine number indicates that the date stone has a good capability to remove most of BTX which have molecular sizes in the range of micropores content [69].

**Table 4.1:** The characteristics of date stones activated carbon.

Sample code	Yeild	Iodine number (IN) mg/g	Surface area from IN m <sup>2</sup> /g	Surface area from BET m <sup>2</sup> /g
AC/ FeCl <sub>3</sub>	39.8%	739.775	694.149	893.780
AC/ AgNO <sub>3</sub>	37.4%	676.275	635.519	818.289
AC/ CuSO <sub>4</sub> ·5H <sub>2</sub> O	42.3%	708.025	664.834	796.028

#### 4.2 SEM Analysis of the AC

SEM has been used to investigate the surface morphology of the prepared date stone activated carbon.



Fig.4.1 shows that many large pores were clearly found on the surface of the activated carbon. This shows that  $\text{FeCl}_3$  was effective in developing pores on the surface of the precursor.

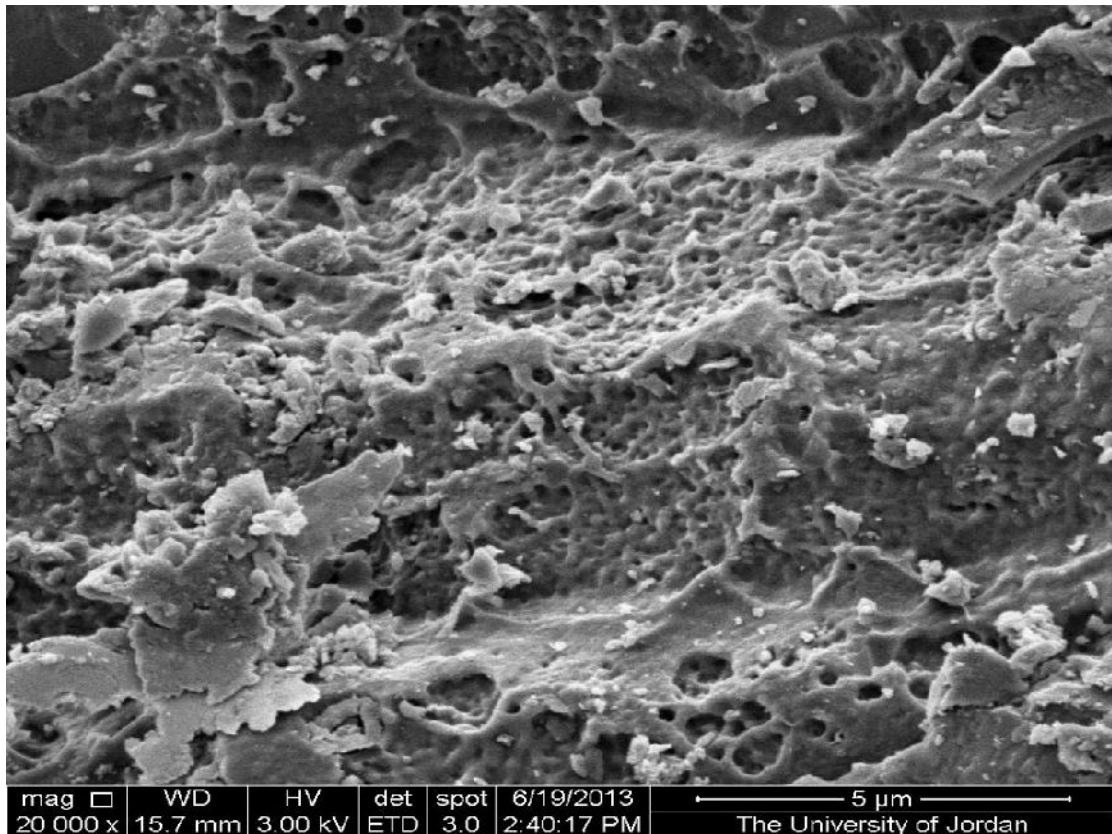


**Figure 4.1:** SEM micrographs of AC/  $\text{FeCl}_3$ .

## 4.4 Adsorption Efficiency of AC

### 4.4.1 Calibration curve for BTX

Different BTX standard solutions with different concentrations were prepared. Then the samples were analyzed by a GC-MS.

Calibration curve were constructed by plotting the value of area under the peak vs. concentration of standard BTX as shown in Fig. 4.2.

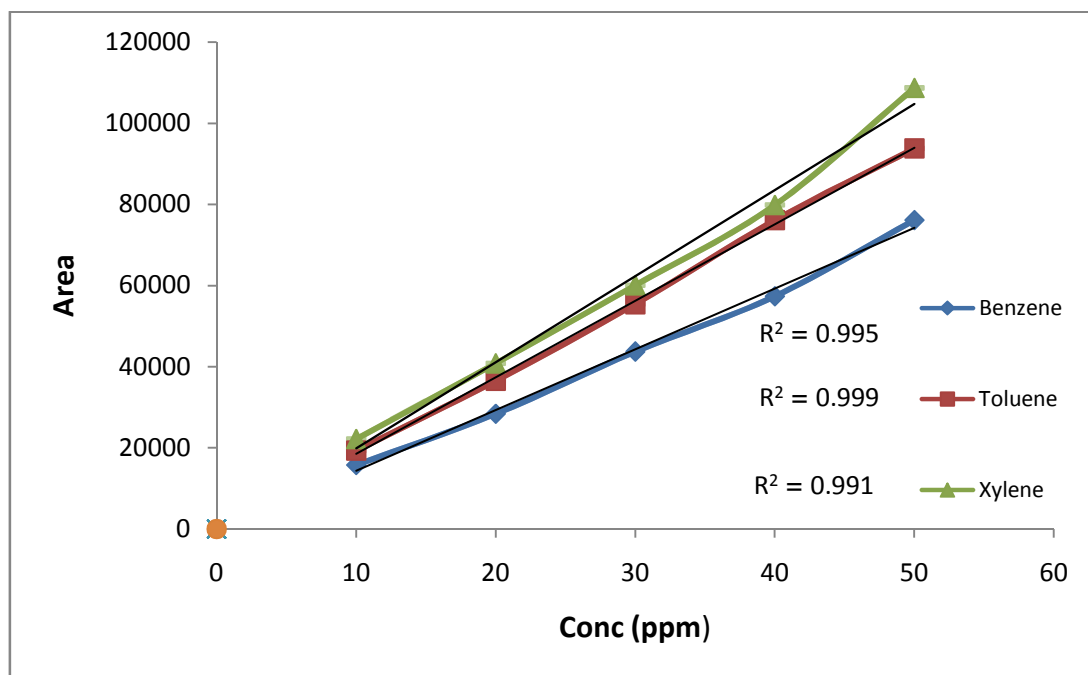


**Figure 4.2:** Calibration curve for BTX standard solutions at 25 °C.

A straight lines was obtained with a correlation factor of 0.995, 0.999 and 0.991 for benzene, toluene and xylene respectively.

#### 4.4.2 Effect of contact time

The effect of contact time on the adsorption of BTX by date stone with  $\text{FeCl}_3$  activating agent was studied at 5-1440 min. The results are shown in Figure 4.3. The Figure shows that BTX adsorption has been rapidly increased for the first 180min. Then the adsorption capacity increases slowly until it reached equilibrium.

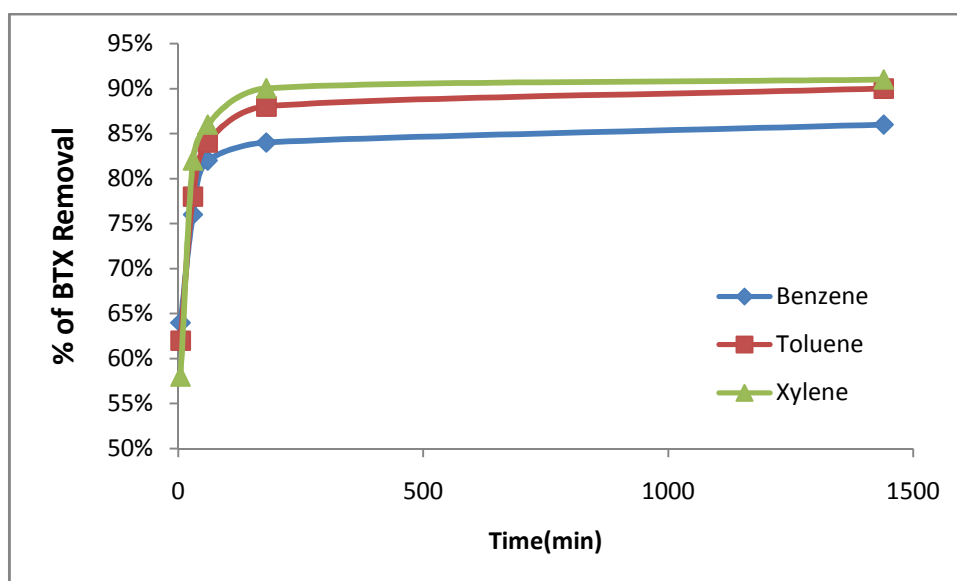


**Figure 4.3:** Effect of contact time on the adsorption of BTX by AC/FeCl<sub>3</sub> at initial concentration 50 ppm, pH: 4, temperature: 25°C and 0.25g of AC.

The fast adsorption at the initial stage may be due to the higher driving force making fast transfer of BTX ions to the surface of date stone particles and the availability of the uncovered surface area and the remaining active sites on the adsorbent [70].

The order of the sorption capacity of the modified adsorbent is B < T < X. This order may be due to the water solubility [71]. Many previous studies have confirmed that the sorption of BTX from aqueous solutions with various adsorbents follows a similar order as above [72, 73, 74].

#### 4.4.3 Effect of Dosage

The range of activated carbon dose which was used is 0.1-1.5 g. The effects of dosage are shown in Figure 4.4.

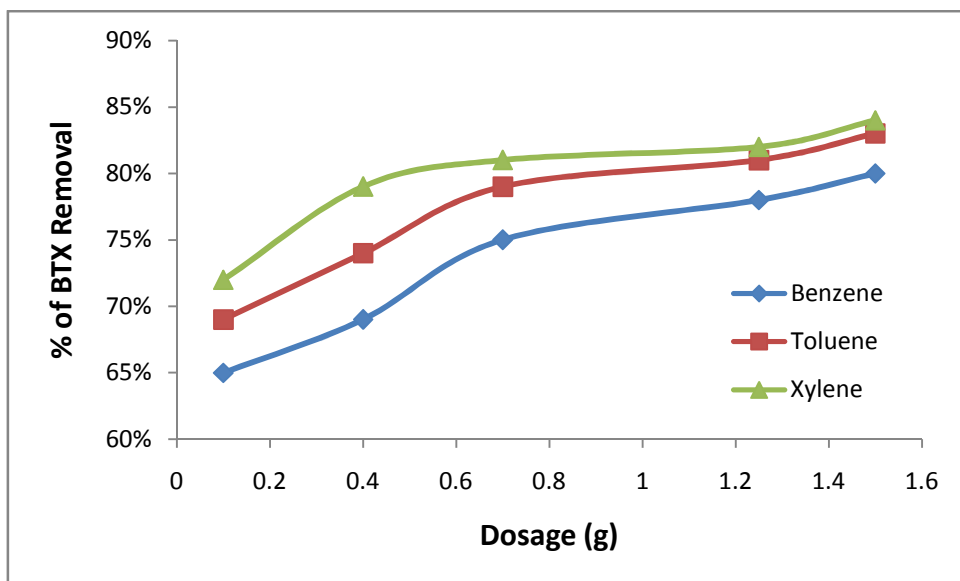


**Figure 4.4:** Effect of AC dosage on the adsorption of BTX by AC/FeCl<sub>3</sub> at initial concentration 50 ppm, pH: 4 and temperature: 25 °C for 30 min.

The amount of BTX removal was increased rapidly until 0.7g of AC and then it increased slowly from 0.8 to 1.5 g.

In the first part, as the amount of AC increased at constant BTX concentration, the adsorption of pollutant increased because it provided more adsorption sites (i.e. more surface area). But in the second part, the adsorption effectiveness was slowed down because most of BTX was adsorbed [75].

#### 4.4.4 Effect of Temperature

This effect was studied at 15-45°C by adding activated carbon to 50 ppm BTX solutions at pH 4 for 30 min. The results are summarized in Fig. 4.5.

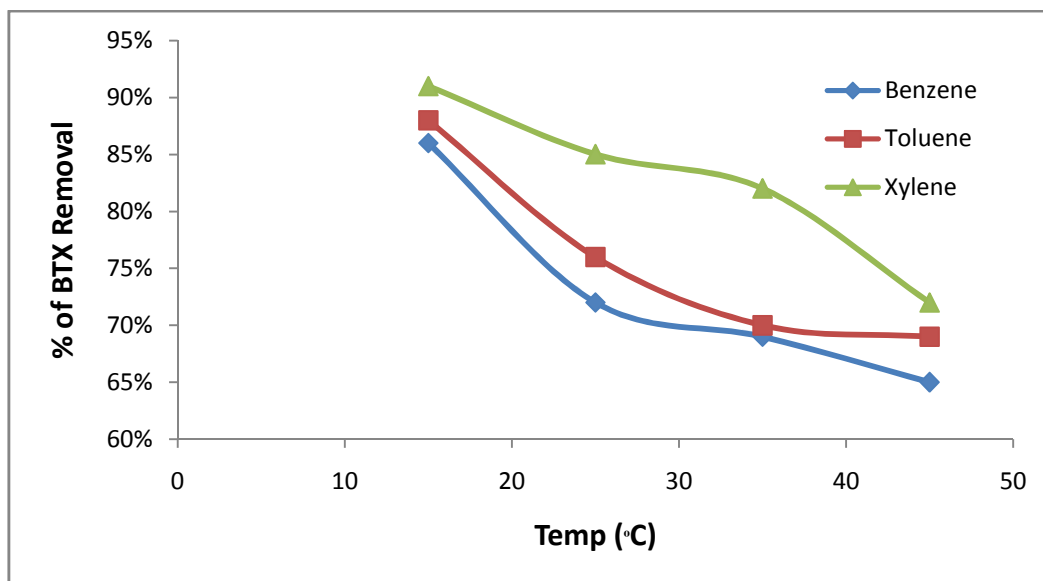


**Figure 4.5:** Effect of temperature on BTX removal by AC/FeCl<sub>3</sub> at initial conc: 50 ppm, pH: 4 and temperature: 25 °C for 30 min.

It can be seen from Fig.4.5 that, as the activation temperature increases, the adsorption effectiveness for BTX decreases. This is due to the loss of the volatile materials and active sites for adsorption at higher temperatures [76,77].

Generally, as temperature increases, the adsorption capacity decreases due to the following reasons:

1. Energy Content: As the temperature raises, the energy content increases, therefore, the adsorbent requires more energy to remain in a liquid state, thus directly affecting the adsorption balance.
2. Saturated Vapour Pressure: As the temperature rises, the vapour pressure increases making it more difficult to keep the adsorbent in its liquid state [78].

#### 4.4.5 Effect of pH

The amount of BTX removal under the influence of pH was investigated in the range 2-10. Figure 4.6 summarizes the results.

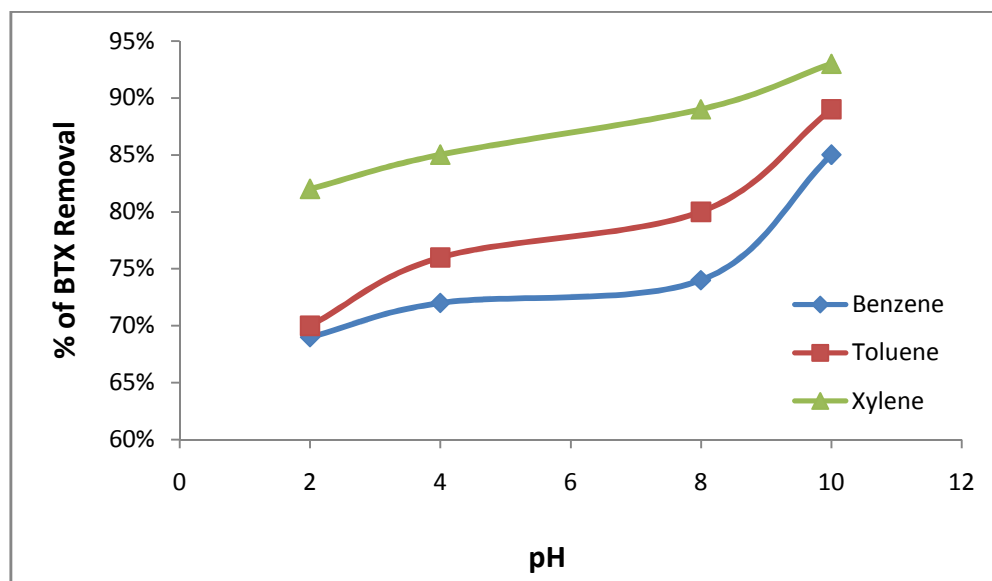


**Figure 4.6:** Effect of pH on the adsorption of BTX by AC/FeCl<sub>3</sub> at initial concentration 50 ppm, 0.25 g of AC and temperature: 25 °C for 30 min.

From the Figure it can be noticed that the amount of BTX removals directly proportional to the degree of pH, and the adsorption value at pH 10 increases up to (85%, 89% and 93%) for (benzene, toluene and xylene) respectively.

As we show in Figure 4.6, the addition of NaOH leads to decreases the solubility of all organic material because NaOH is more soluble in water, which means increases the adsorption of benzene, toluene and xylene, due to the salting out effect [73].

## 4.5 Adsorption Isotherm

The study of adsorption isotherm is important to determine the adsorption capacity of BTX by date stone activated carbon.

In order to achieve this, the data were fitted to Langmuir and freundlich isotherms which describe the relationship between the amounts of BTX adsorbed and its equilibrium concentration in solution.

The adsorption parameters were investigated by plotting  $C_e/q_e$  vs.  $C_e$  for Langmuir Eq.(2.1) and  $\log q_e$  vs.  $\log C_e$  for Freundlich Eq.(2.2) as shown in Fig. 4.7.a, b, c and Fig. 4.8.a,b,c respectively.

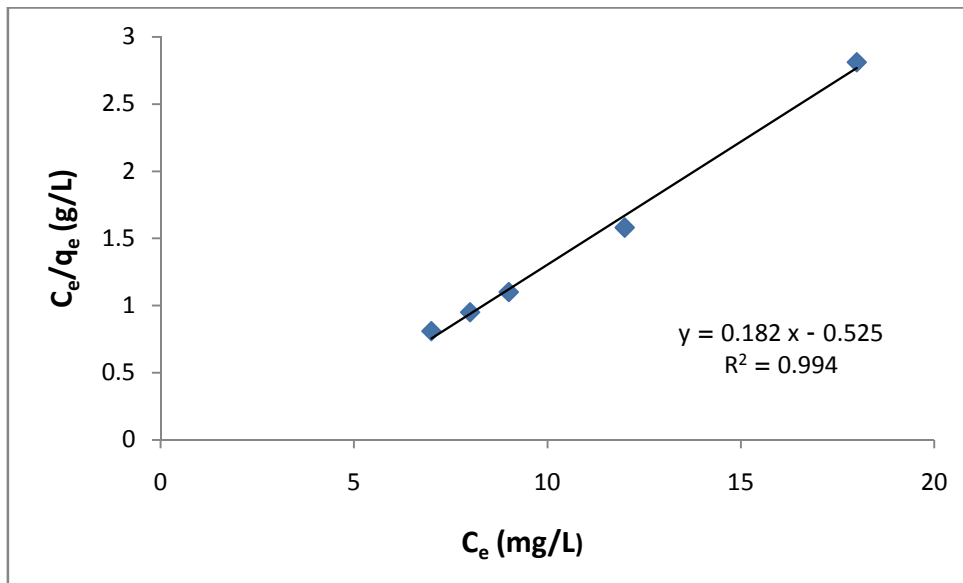


**Figure 4.7.a:** Langmuir plot for benzene adsorption onto AC/FeCl<sub>3</sub> at temperature: 25 °C, pH: 4 and solid/liquid ratio 0.25 g/50 mL.

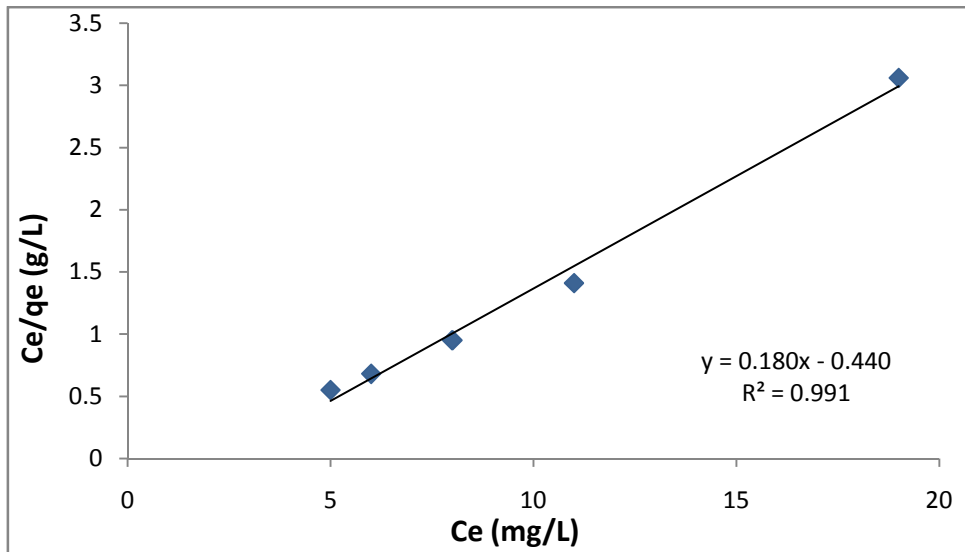


**Figure 4.7.b:** Langmuir plot for toluene adsorption onto AC/FeCl<sub>3</sub> at temperature: 25 °C, pH: 4 and solid/liquid ratio 0.25 g/50 mL.

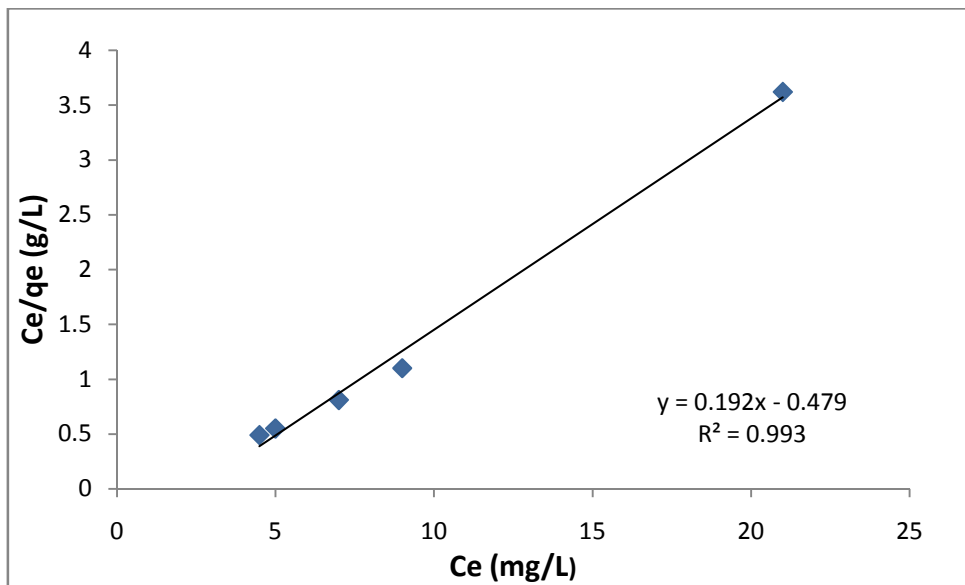


**Figure 4.7.c:** Langmuir plot for xylene adsorption onto AC/FeCl<sub>3</sub> at temperature: 25 °C, pH: 4 and solid/liquid ratio 0.25 g/50 mL.



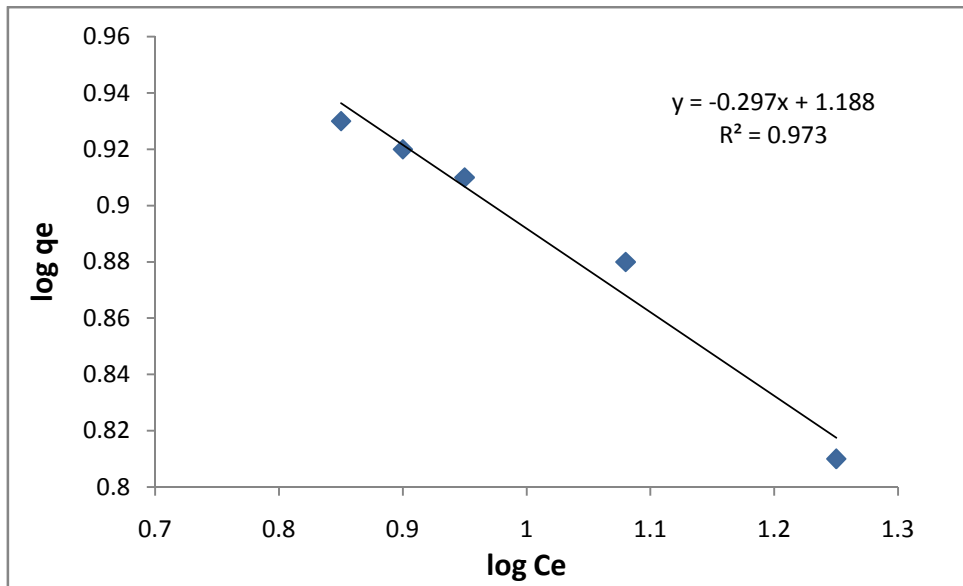


**Figure 4.8.a:** Freundlich plot for benzene adsorption onto AC/FeCl<sub>3</sub> at temperature: 25 °C, pH: 4 and solid/liquid ratio 0.25 g/50 mL).

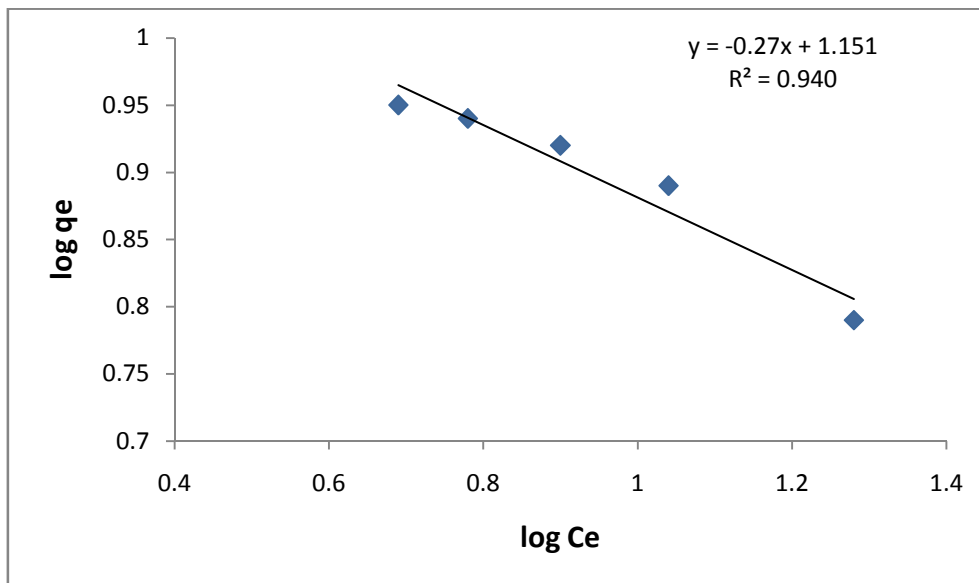


**Figure 4.8.b:** Freundlich plot for toluene adsorption onto AC/FeCl<sub>3</sub> at temperature: 25 °C, pH: 4 and solid/liquid ratio 0.25 g/50 mL).

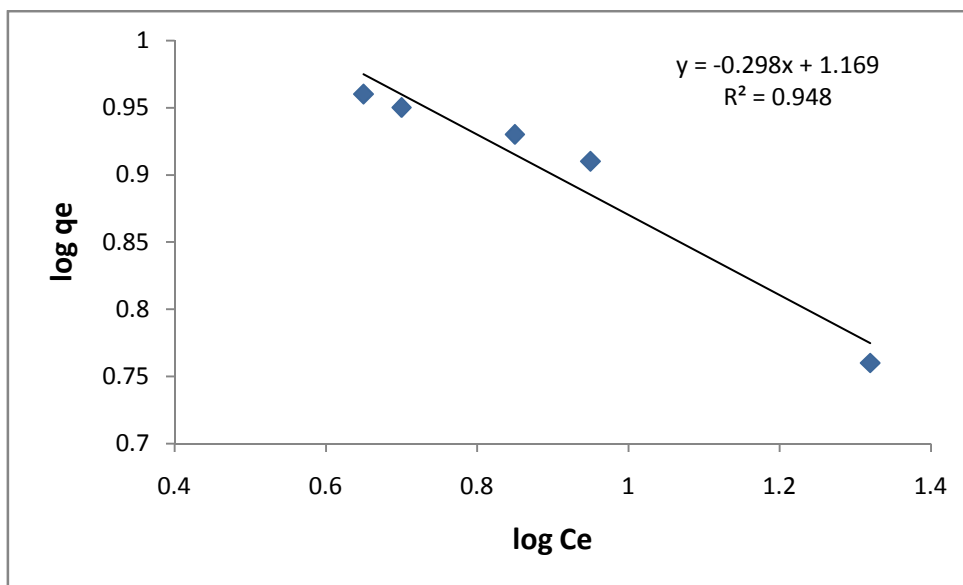


**Figure 4.8.c:** Freundlich plot for xylene adsorption onto AC/FeCl<sub>3</sub> at temperature: 25 °C, pH: 4 and solid/liquid ratio 0.25 g/50 mL).

The adsorption isotherm parameters and correlation coefficients which were found from the slope and intercept are summarized in Table 4.2.

**Table 4.2<sup>2</sup>:** Langmuir and Freundlich isotherm parameters and correlation coefficient of BTX adsorption onto AC/FeCl<sub>3</sub>.

Isotherm	Langmuir			Freundlich		
	Parameters		R <sup>2</sup>	Parameters		R <sup>2</sup>
Adsorbate	q <sub>0</sub> (mg/g)	b (L/mg)		K <sub>f</sub> ((mg/g)(L/mg) <sup>1/n</sup> )	n	
Benzene	5.47	-0.35	0.995	15.44	- 3.37	0.973
Toluene	5.53	-0.41	0.992	14.16	- 3.70	0.940
Xylene	5.19	-0.40	0.993	14.76	- 3.35	0.948

Freundlich adsorption equation is perhaps the most widely used in mathematical description of adsorption in aqueous systems and describes equilibrium adsorption on heterogeneous surfaces and hence does not

<sup>2</sup>The calculations are shown in appendix A.2, sections A.2.1 and A.2.2.

assume monolayer, while the Langmuir adsorption isotherm is commonly applied to monolayer physisorption of gases onto a uniform adsorbent surface [79].

As shown in Table 4.2, the correlation coefficients in Langmuir adsorption isotherm are very high and closer to one than in freundlich.

In Freundlich isotherm,  $n$  value giving an indication of how the adsorption process is suitable. Adsorption process is considered as beneficial when  $n$  value is between 1 and 10, which means stronger interaction between the adsorbent and the adsorbate [80]. A value for  $(n)$  below one indicates a normal Langmuir isotherm, while  $(n)$  above one is indicative of efficient adsorption [80]. In this study, the calculated  $n$  value as shown in Table 4.2.

As a conclusion, the adsorption of BTX follows Langmuir isotherm in this study.

#### **4.6 Kinetics of adsorption**

The experimental kinetic data for BTX adsorption on date stones are fitted with pseudo-first order, pseudo-second order and intraparticle diffusion models, Eqs. (2.3)-(2.5), In order to investigate the mechanism of BTX adsorption process.

The kinetics parameters and correlation coefficients at 50 mg/L initial adsorbate concentration have been calculated from the linear plots of log

$(q_e - q_t)$  versus  $t$  and  $t/q_t$  versus  $t$ , Figure 4.9 and Figure 4.10 respectively and the results are presented in Table 4.3.

The data show large difference between the experimental and calculated adsorption capacity ( $q_e$ ) for BTX on the pseudo-first order model and good agreement based on the pseudo-second order model. On the other hand, the correlation coefficient of the pseudo-second order model was larger than for pseudo-first order model, indicating a poor pseudo-first order to fit the experimental data.

This suggests that the pseudo-second order is better to describe the mechanism of BTX adsorption process by date stone activated carbon.

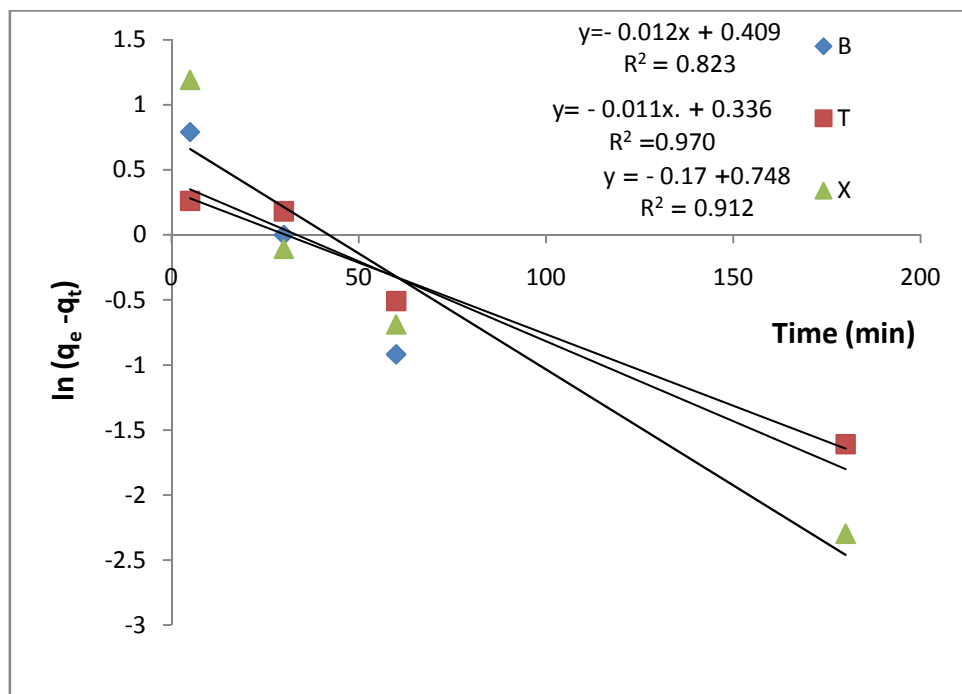


**Figure 4.9:** Kinetics of BTX removal according to the pseudo-first-order model by AC/FeCl<sub>3</sub> at temperature: 25 °C, pH: 4 and solid/liquid ratio 0.25 g/50 mL).

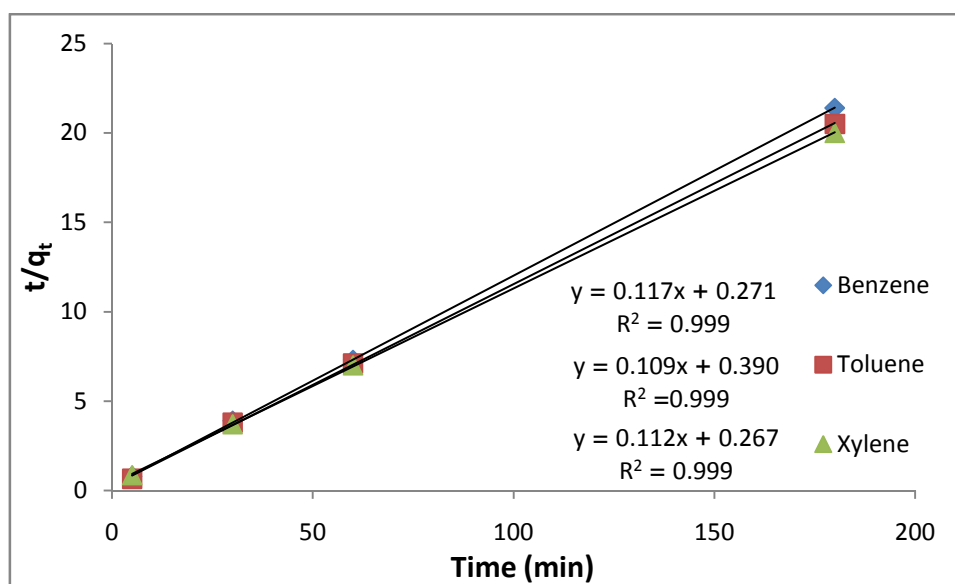


**Figure 4.10:** Kinetics of BTX removal according to the pseudo-second-order model by AC/FeCl<sub>3</sub> at temperature: 25 °C, pH: 4 and solid/liquid ratio 0.25 g/50 mL).

**Table 4.3<sup>3</sup>:** Pseudo-first-order and pseudo-second-order kinetic model parameters for BTX adsorption by AC/ FeCl<sub>3</sub>.

Adsorbent	q <sub>e</sub> (exp) (mg/g)	Pseudo-first order kinetic model		R <sup>2</sup>	Pseudo-second order kinetic model		R <sup>2</sup>
		k <sub>1</sub> (min- 1)	q <sub>e</sub> (calc) (mg/g)		k <sub>2</sub> (g/mg.min)	q <sub>e</sub> (calc) (mg/g)	
Benzene	8.6	0.0123	1.51	0.8231	0.0507	8.52	0.9999
Toluene	9.0	0.0110	1.40	0.9704	0.0305	9.17	0.9999
Xylene	9.1	0.0178	2.11	0.9127	0.0475	8.87	0.9997

For the intraparticle diffusion model Eq. (2.5), the q<sub>t</sub> values are calculated by using the Equation 3.3. The values of K<sub>i</sub> and A are found from the slope and the intercept of the linear plot of q<sub>t</sub> versus t<sup>0.5</sup>. The results are shown in Figure 4.11, Table 4.4 and Table 4.5.

<sup>3</sup>The calculations are shown in appendix A.3, sections A.3.1 and A.3.2.

**Table 4.4<sup>4</sup>:** The values of  $q_t$  and  $t^{0.5}$  for intra-particle diffusion kinetic model.

$t^{0.5}$	$q_t$		
	Benzene	Toluene	Xylene
2.24	6.4	7.75	5.8
5.48	7.6	7.8	8.2
7.75	8.2	8.4	8.6
13.42	8.4	8.8	9

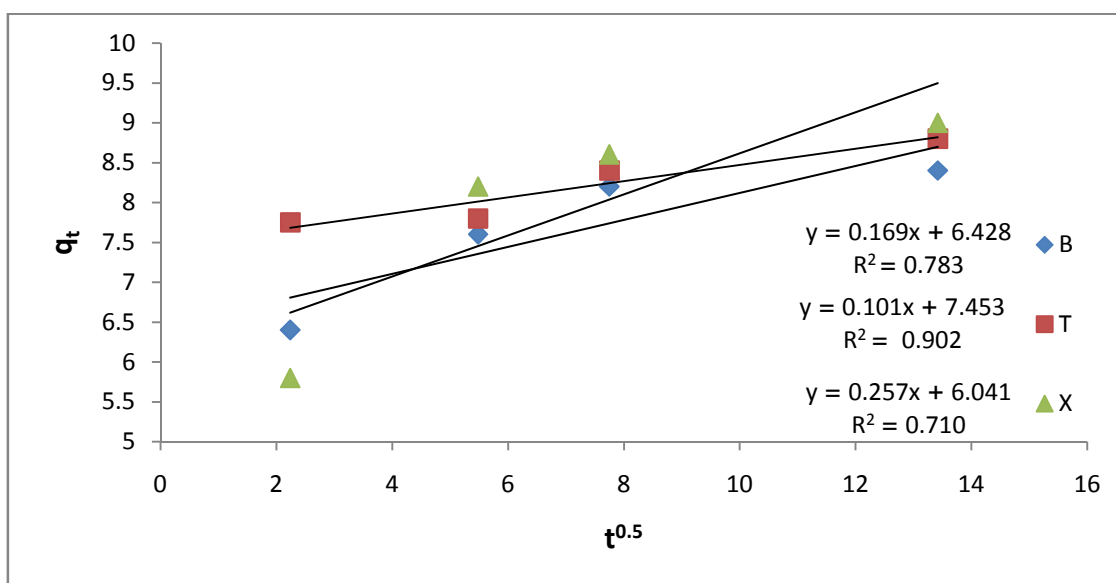


**Figure 4.11:** Kinetics of BTX removal according to the intra-particle diffusion model by AC/FeCl<sub>3</sub> at temperature: 25°C, pH: 4 and solid/liquid ratio 0.25 g/50 mL).

**Table 4.5<sup>5</sup>:** Intra-particle diffusion kinetic model parameters for BTX adsorption by AC/ FeCl<sub>3</sub>.

Adsorbent	$K_i$ (mg/g min <sup>1/2</sup> )	A	$R^2$
Benzene	0.1691	6.728	0.7831
Toluene	0.1016	7.4535	0.9021
Xylene	0.2574	6.0412	0.7109

<sup>4</sup>The calculations are shown in appendix A.3, section A.3.3.

<sup>5</sup>The calculations are shown in appendix A.3, section A.3.3.

The intraparticle diffusion model is used to describe the diffusion mechanism. If the straight lines did not pass through the origin, this indicates that the rate is limited by mass transfer across the boundary layer and the mechanism of removal is complex [81]. While the value of A give an information about the thickness of the boundary layer.

#### 4.7 Adsorption Thermodynamics

According to Equation (2.6), the  $\Delta H^\circ$ ,  $\Delta S^\circ$  parameters for BTX can be calculated from the slope and intercepts of the plot of  $\ln K_d$  versus  $1/T$  respectively (Fig. 4.12), and  $\Delta G^\circ$  values are obtained from the Equation (2.8). While the values of  $K_d$  calculated by using Equation (2.7). The obtained values of  $\Delta H^\circ$ ,  $\Delta S^\circ$  and  $\Delta G^\circ$  are listed in Table 4.5.

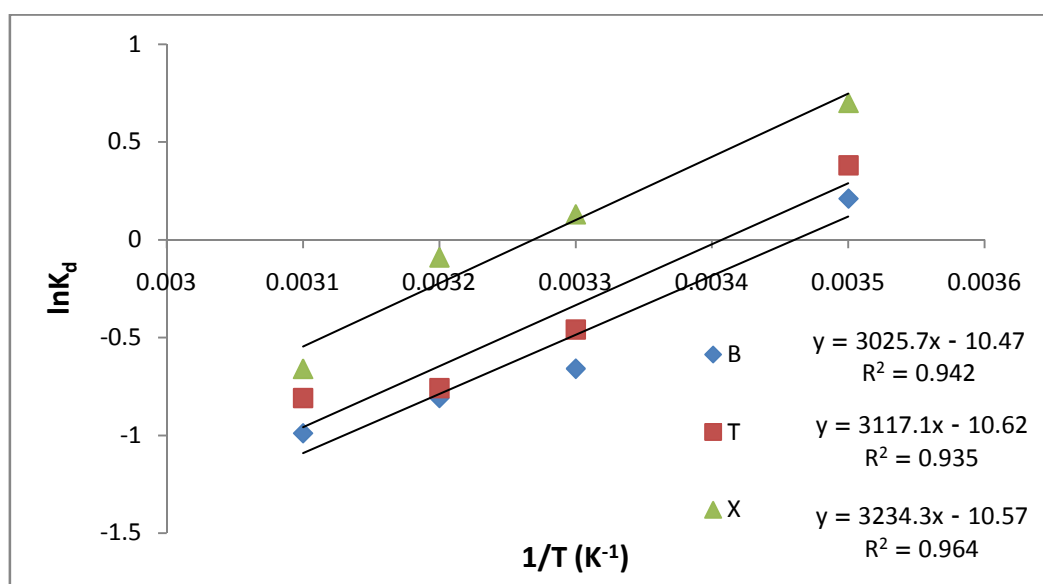


**Figure 4.12:** Plot of  $\ln K_d$  versus  $1/T$  for BTX adsorption on AC/  $\text{FeCl}_3$ .

**Table 4.6<sup>6</sup>:** The values of the thermodynamic of adsorption at various temperatures and various adsorbents.

Adsorbent	$\Delta H^\circ$ (kJ/mol)	$\Delta S^\circ$ (J/mol K)	$\Delta G^\circ$ (kJ/mol)			
			288 K	298 K	308 K	318 K
Benzene	-25.16	-87.06	-0.50	1.58	1.94	2.37
Toluene	-25.91	-88.30	-0.90	1.14	1.95	2.14
Xylene	-26.89	-87.89	-1.68	-3.22	0.23	1.74

The negative values of enthalpy ( $\Delta H^\circ$ ) indicate that the nature of the adsorption is exothermic and its magnitude gives information on the type of adsorption, which can be either physical or chemical adsorption.

Furthermore, the negative values of entropy ( $\Delta S^\circ$ ) show that the decrease in the randomness at sorbate-solution interface during the adsorption process.

A negative  $\Delta G^\circ$  value means the reaction is favorable. Increase in the value of  $\Delta G^\circ$  with rise in temperature show that the adsorption is more favorable at lower temperature.

---

<sup>6</sup>The calculations are shown in appendix A.4.



## Conclusion

The results that have been obtained in this work can be summarized in the following points:

1. Using of activated carbon produced from date stones to remove the BTX from water is good and efficiency method.
2. Date stones have high surface area which means that the use of it for the removal of BTX from aqueous solutions is successfully.
3. The values of surface area showed that the using  $\text{FeCl}_3$  as activating agent for date stones is better than  $\text{CuSO}_4 \cdot 5\text{H}_2\text{O}$  and  $\text{AgNO}_3$ .
4. The results showed that the adsorption of BTX by date stones activated carbon increase by increasing time, dosage and pH.
5. The results indicate that the adsorption effectiveness was increased with decreasing temperature.
6. Adsorption of BTX by AC/ $\text{FeCl}_3$  followed Langmuir isotherm.
7. Experimental data showed that BTX adsorption can be represented by pseudo- second order model.
8. Intraparticle model which describe the diffusion mechanism showed that the mass transfer happen across the boundary layer.

9. The results of  $\Delta H^\circ$ ,  $\Delta S^\circ$  and  $\Delta G^\circ$  show that the adsorption of BTX by AC/  $\text{FeCl}_3$  is exothermic and favorable process.

10. The adsorption of BTX by  $\text{FeCl}_3$  is physical adsorption.

## **Suggestions for Future Work**

Recommendations that can be forwarded in this study are as follows:

1. Producing activated carbon by impregnated it with different solutions.
2. Study the effect of contact time, amount of dose, pH and temperature on the activated carbon effectiveness of activated carbon which impregnated with  $\text{AgNO}_3$  and  $\text{CuSO}_4 \cdot 5\text{H}_2\text{O}$ .
3. Using different type of polymer like polymer synthesis from cellulose instead of activated carbon produced from date stone palm pits.
4. Using different technique of nanoparticle from natural fiber for adsorption/ degradation of BTX from water.
5. Grinding the prepared activated carbon to mesh number less than 16 to increase the surface area.

## References

- [1] T. Ahmad, M. Danish, M. Rafatullah, A. Ghazali, O. Sulaiman, R. Hashim, M. Ibrahim. *The use of date palm as a potential adsorbent for wastewater treatment*. *Env. Sci. and Pollution Res.*, 19 (2012) 1464-1484.
- [2] D. Pink. *Investing in Tomorrow's Liquid Gold*, *Asian. J. Exp. Sci.*, 23 (2006) 61-66.
- [3] H. Hettige, M. Huq, S. Pargal, D. Wheeler. *Determinants of pollution abatement in developing countries: evidence from south and Southeast Asia*. *World Develop*, 24 (1996) 1891–1906.
- [4] G. Vassalli, S. Proezion. *Analysis of BTEX in Natural Water with SPME*. *Agilent Technologies*, 251 (2010) 231-237.
- [5] A. Daifullah, B. Girgis. *Impact of surface characteristics of activated carbon on adsorption of BTEX*. *Colloids and surfaces A*, 214 (2003) 181-193.
- [6] J. Smith, S. Bartelt-Hunt, S. Burns. *Sorption and permeability of gasoline hydrocarbons in organobentonite porous media*. *J. of Hazardous Materials*, 96 (2003) 91-97
- [7] E. Tiburtius, P. Peralta-Zamora, A. Emmel. *Treatment of gasoline-contaminated waters by advanced oxidation process*. *J. of Hazardous Materials*, 126 (2005) 86-90.

- [8] M. Aivalioti, I. Vamvasakis, E. Gidakos. *BTEX and MTBE adsorption onto raw and thermally modified diatomite*, J. of Hazardous Materials, 178 (2010) 136-143.
- [9] F. Rodrieguez-Reinoso. *Activated carbon: Structure, characterization, preparation and applications. Introduction to carbon technologies(dissertation)*. Universidad de Alicante, Spain, (1997) 60.
- [10] W. Melchert, C. Infante , F. Rocha. *Activated carbon manufacture, structure & properties*. Cameron Carbon, USA, (2006) 394-405.
- [11] M. Al-Ghouti MA, J. Li, Y. Salamh, N. Al-Laqtah, G. Walker, M. Ahmad. *Adsorption mechanisms of removing heavy metals and dyes from aqueous solution using date pits solid adsorbent*. J. of Hazardous Materials, 176 (2010) 510–520.
- [12] A. El-Hendawy. *The role of surface chemistry and solution pH on the removal of Pb<sup>2+</sup> and Cd<sup>2+</sup> ions via effective adsorbents from low-cost biomass*. J. of Hazardous Materials 167 (2009) 260–267.
- [13] S. Ashour. *Kinetic and equilibrium adsorption of methylene blue and remazol dyes onto steam-activated carbons developed from date pits*. J. Saudi Chem. Soc., 14 (2010) 47–53.
- [14] A. Okasha, H. Ibrahim. *Phenol removal from aqueous systems by sorption of using some local waste materials*. Elec. J. of Envi., 9 (2010) 796–807.

- [15] M. Danish M, O. Sulaiman, M. Rafatullah, R. Hashim, A. Ahmad. ***Kinetics for the removal of paraquat dichloride from aqueous solution by activated date (Phoenix dactylifera) stone carbon.*** J. of Dispersion Science and Technology, 31 (2010) 248-259.
- [16] S. Ashour. **Adsorption of herbicide (pendimethalin) onto activated carbons developed from date pits.** Egyptian J Chem., 51 (2008) 55–67.
- [17] M. El-Naas, S. Al-Zuhair, M. Alhaija. ***Reduction of COD in refinery wastewater through adsorption on date-pit activated carbon.*** J. of Hazard. Mater., 173 (2010) 750–757.
- [18] M. Kamil, M. Naji. ***Use of bio-pesticide- new dimension and challenges for sustainable date palm production.*** In IV International Date Palm Conference, 882, (1995) 50-56.
- [19] L. Boughediri, N. Bounaga. ***In vitro germination of date pollen and its relation to fruit set.*** Date Palm J., 5 (1987) 120 - 127.
- [20] J. Capinera. ***Encyclopedia of Entomology.*** Springer, USA, 3 (2008) 4346.
- [21] K. Ramakrishna, T. Viraraghavan. ***Dye removal using low cost adsorbents.*** Water Sci. and Tech., 36 (1997) 189-196.
- [22] b. Jibril, O. Houache, R. Al-Maamari, B. Al-Rashidi. ***Effects of H<sub>3</sub>PO<sub>4</sub> and KOH in carbonization of lignocellulosic material.*** J. Anal. Appl. Pyrolysis, 83 (2008) 151–156.

- [23] A. Reffas, V. Bernardet, B. David, L. Reinert, M. Lehocine, M. Dubois, N. Batische, L. Duclaux. *Carbons prepared from coffee grounds by  $H_3PO_4$  activation: Characterization and adsorption of methylene blue and Nylosan Red N-2RBL*. J. Hazardous Materials, 175 (2010) 779-788.
- [24] R. Baccar, J. Bouzid, M. Feki, A. Montiel. *Preparation of activated carbon from Tunisian olive-waste cakes and its application for adsorption of heavy metal ions*. J. of Hazardous Materials, 162 (2009) 1522-1529.
- [25] T. Yang, A. Lua, *Textural and chemical properties of zinc chloride activated carbons prepared from pistachio-nut shells*, Materials Chemistry and Physics, 100 (2006) 438-444.
- [26] D. Kalderis, S. Bethanis, P. Paraskeva, E. Diamadopoulos. *Production of activated carbon from bagasse and ricehusk by a single stage chemical activation method at low retention times*. J. Bioresource Technol., 99 (2008) 6809-6816.
- [27] A. Mestre, J. Pires, J. Nogueira, J. Parra, A. Carvalho, C. Ania. *Waste derived activated carbons for removal of ibuprofen from solution: role of surface chemistry and pore structure*. J. Bioresource Technology, 100 (2009) 1720-1726.
- [28] H. Marsh, F. Reinoso. *Activated Carbon*. Elsevier, UK (2006) 237.

- [29] J. Kim, M. Sohn, D. Kim, S. Sohn Y. Kwon. *Production of granular activated carbon from waste walnut shell and its adsorption characteristics for Cu<sup>2+</sup> ion*. J. Hazard Mater., 85 (2001) 301-312.
- [30] N. Yalcin, V. Sevinc. *Studies of the surface area and porosity of activated carbons prepared from rice husks*. Carbon, 38 (2000) 1943-1950.
- [31] G. Bello, R. Cid, R. Garcia, J. Arriagada. *Retention of Cr(VI) and Hg(II) in Eucalyptus globulus- and peach stone-activated carbons*. Chem. Technol. Biotechnol., 74 (1999) 904-911.
- [32] B. Girgis, L. Khalil, T. Tawfik. *Activated carbon from sugar cane bagasse by carbonization in the presence of inorganic acids*. Chem. Technol. Biotechnol., 61 (1994) 87-92.
- [33] C. Namasivayam, K. Kadirvelu. *Activated carbons prepared from coir pith by physical and chemical activation methods*. Bioresource Technol., 62 (1997) 123-130.
- [34] K. Periasamy, C. Namasivayam. *Process Development for Removal and Recovery of Cadmium from Wastewater by a Low-Cost Adsorbent: Adsorption Rates and Equilibrium Studies*. Ind. Eng. Chem. Res., 33 (1994) 317-325.
- [35] T. Kopac, A. Toprak. *Preparation of activated carbons from Zonguldak region coals by physical and chemical activations for*

*hydrogen sorption*. International Journal of Hydrogen Energy, 32 (2007) 5005- 5014.

[36] C. Bouchelta, M. Medjram, O. Bertrand, J. Bellat. *Preparation and characterization of activated carbon from date stones by physical activation with steam*. Journal of Analytical and Applied Pyrolysis , 82 (2008) 70-77.

[37] S. Román, J. González, C. González-García , F. Zamora. *Control of pore development during CO<sub>2</sub> and steam activation of olive stones*. Fuel Processing Technology, 89 (2008) 715-720.

[38] T. Al-Khalid, N. Haimour, S. Sayed, B. Akash. **Activation of olive-seed waste residue using CO<sub>2</sub> in a fluidized-bed reactor**, Fuel Processing Technology, 57 (1998) 55-64.

[39] [http://www.safe.nite.go.jp/english/ghs\\_index.htm](http://www.safe.nite.go.jp/english/ghs_index.htm) (3 August 2013).

[40] M. Ahmed. *Preparation of Activated Carbons from Date Stones by Chemical Activation Method Using FeCl<sub>3</sub> and ZnCl<sub>2</sub> as Activation Agents*. Journal of Engineering, 17 (2011) 19-24.

[41] L. Oliveira, E. Pereira, I. Guimaraes, K. Sapag. *Preparation of activated carbons from coffee husks utilizing FeCl<sub>3</sub> and ZnCl<sub>2</sub> as activating agents*. J. of Hazardous Materials, 165 (2009) 87- 94.

[42] T. Rufford, D. Hulicova-Jurcakova, Z. Zhu, G. Lu. *A comparative study of chemical treatment by FeCl<sub>3</sub>, MgCl<sub>2</sub>, and ZnCl<sub>2</sub> on*



*microstructure, surface chemistry, and double-layer capacitance of carbons from waste biomass*. J. of Material Research, 25 (2010) 1451-1459.

[43] P. Meyer, A. Rimsky, R. Chevalier. *Structure of Silver-Nitrate Phase Unstable at Ordinary Temperature and Pressure*. Acta Crystallographica Section B-Structural Science, 15 (1976) 1143-1146.

[44] <http://www.taylorgeoservices.com/papers/point%20system.PDF> (19 September 2013).

[45] [http://en.wikipedia.org/wiki/Copper\(II\)\\_sulfate](http://en.wikipedia.org/wiki/Copper(II)_sulfate) (28 November 2013).

[46] R. Donnell, J. Christian. *Forensic Investigation of Clandestine Laboratories*. CRC Press, USA (2003) 392.

[47] G. Bacon, D. Titterton. *Neutron-diffraction studies of  $\text{CuSO}_4 \cdot 5\text{H}_2\text{O}$  and  $\text{CuSO}_4 \cdot 5\text{D}_2\text{O}$* . Z. Kristallogr, 141 (1975) 330–341.

[48] J. Kopka. Gas chromatography mass spectrometry. Springer Berlin Heidelberg, 57 (2006) 3-20.

[49] A. Vaikkinen. *Direct Open Air Surface Sampling/Ionization Mass Spectrometry Methods in the Study of Neutral and Nonpolar Compounds (dissertation)*. University of Helsinki, Finland (2013) 60.

[50] M. Lee, C. Chang, J. Dou. *Determination of benzene, toluene, ethylbenzene, xylenes in water at sub-ng l<sup>-1</sup> levels by solid-phase*

*microextraction coupled to cryo-trap gas chromatography–mass spectrometry. Chemosphere*, 69 (2007) 1381-1387.

[51] J. Pawliszyn. *Solid Phase Microextraction: Theory and Practice*. Wiley-Vch, New York, 61 (1997) 264.

[52] Z. Zhang, M. Yang. *Determination of BTEX in Water By SPME-GC/MS*. *J. Anal. Chem.*, 66 (1994) 2.

[53] O. Aly, S. Faust. *Studies on the fate of 2,4-D and ester derivatives in natural surface water*. *J. Agric. Food Chem.*, 12 (1964) 541-546.

[54] M. Panayotova. *Kinetics and thermodynamics of copper ions removal from wastewater by use of zeolite*. *Waste Management*, 21 (2001) 671-676.

[55] M. Ugurlu, A. Gurses, C. Dogar. *Adsorption studies on the treatment of textile dyeing effluent by activated carbon prepared from olive stone by ZnCl<sub>2</sub> activation*, *J. of Color. Technol.*, 123 (2007) 106-114.

[56] G. McKay. *Use of adsorbents for the removal of pollutants from waste waters*. CRC, USA (1995) 208.

[57] A. Agrawal, K. Sahu. *Kinetics and isotherm studies of cadmium adsorption on manganese nodule residue*. *Journal of Hazardous Materials*, 137 (2006) 915-924.

- [58] Y. Li, S. Wang, Z. Luan, J. Ding, C. Xu, D. Wu. *Adsorption of Cadmium (II) from aqueous solution by surface oxidized carbon nanotubes*. J. of Elsevier, 41 (2003) 1057–1062.
- [59] J. Lin, L. Wang. *Comparison between linear and non-linear forms of pseudo-first-order and pseudo-second-order adsorption kinetic models for the removal of methylene blue by activated carbon*. J. of Environ Sci Engin., 83 (2009) 11-17.
- [60] M. Ugurlu, A. Gurses, M. Acıkyıldız. *Comparison of textile dyeing effluent adsorption on commercial activated carbon and activated carbon prepared from olive stone by  $ZnCl_2$  activation*. Microporous and Mesoporous Materials, 111 (2008) 228-235.
- [61] E. Elmolla, M. Chaudhuri. *Improvement of biodegradability of synthetic amoxicillin wastewater by Photo-Fenton process*. World Applied Science Journal, 5 (2009) 53-58.
- [62] I. Tan, B. Hameed, A. Ahmad. *Equilibrium and Kinetic studies on basic dye adsorption by oil palm fiber activated carbon*, J. Chem. Eng., 127 (2007) 111-119.
- [63] S. Dhidan. *Removal of phenolic compounds from aqueous solutions by adsorption onto activated carbon prepared from date stone by chemical activation with  $FeCl_3$* . Journal of Engineering, 18 (2012) 63-77.

- [64] N. Basalat. *Treatment of Organic Phenolic Contaminant In wastewater Using Activated Carbon From Cypress Products* (dissertation). An-Najah National University, Nablus, Palestine (2012) 71.
- [65] W. McMillan, E. Teller. *The Assumptions of the B.E.T. Theory*. *J. Phys. Chem.*, 55 (1951) 17-20.
- [66] A. Zeller, *Measuring the specific surface area of gas hydrates* (dissertation). University of Gottingen, German (2004) 63.
- [67] D. McMullan, **Scanning electron microscopy**. *Scanning*, 17 (1995) 175–185.
- [68] Q. Lu, G. Sorial. *The effect of functional groups on oligomerization of phenolics on activated carbon*. *J. Hazard. Mater.*, 148 (2007) 436-445.
- [69] M. Aroua, S. Leong, L. Teo, W. Daud. *Real time determination of kinetics of adsorption of lead (II) onto shell based activated carbon using ion selection electrode*, *Bioresou. Technol.*, 99 (2008) 5786-5792.
- [70] F. Su, C. Lu, S. Hu. *Adsorption of benzene, toluene, ethylbenzene and p-xylene by NaOCl-oxidized carbon nanotubes*. *Colloids and Surfaces A: Physicochemical and Engineering Aspects*, 353 (1), (2010), 83–91.
- [71] M. Aivalioti, I. Vamvasakis, E. Gidarakos. *BTEX and MTBE adsorption onto raw and thermally modified diatomite*, *Journal of Hazardous Materials*, 178 (2010) 136–143.

- [72] M. Aivalioti, P. Papoulias, A. Kousaiti, E. Gidarakos. *Adsorption of BTEX, MTBE and TAME on natural and modified diatomite*. Journal of Hazardous Materials, 207 (2012) 117–127.
- [73] A. Daifullah, B. Girgis. **Impact of surface characteristics of activated carbon on adsorption of BTEX**. Colloids and Surfaces A: Physicochemical and Engineering Aspects, 214 (2003) 181–193.
- [74] T. Kopac. *Non-isobaric adsorption analysis of SO<sub>2</sub> on molecular sieve 13X and activated carbon by dynamic technique*. Chemical Engineering and Processing: Process Intensification, 38 (1999) 45-53.
- [75] M. Al-Anber, Z. Al-Anber. *Utilization of natural zeolite as ion-exchange and sorbent material in the removal of iron: Magnetic Study*. Asian J. Chem., 19 (2007) 3493-3501.
- [76] J. Yun, D. Choi, S. Kim. *Equilibria and dynamics for mixed vapors of BTX in an activated carbon bed*. AIChE J, 45 (1999) 751–760.
- [77] <http://www.clarimex.com/p-gaseosa-i.html>. (8 April 2013).
- [78] Sh. Jodeh. *The study of kinetics and thermodynamics of selected pharmaceuticals and personal care products on agriculture soil*. European Journal of Chemistry, 3 (2012) 468-474.
- [79] N. Öztürk, T. Bektas. *Nitrate removal from aqueous solution by adsorption onto various materials*. J. Hazardous Materials, 112 (2004) 155-162.

[80] K. Fytianos, E. Voudrias, E. Kokkalis. *Sorption-desorption behavior of 2,4-dichlorophenol by marine sediments*. Chemosphere, 40, (2000) 3–6.

[81] J. Oppel, G. Broll, D. Löffler, M. Meller, J. Römbke, T. Ternes, *Leaching behaviour of pharmaceuticals in soil-testing-systems: apart of an environmental risk assessment for groundwater protection*. Science of the Total Environment, 328, (2004) 265–273.

## Appendix A

### A.1 The Peak Area

The values of the peak area for the calibration curve are shown in the following table:

Concentration (ppm)	Peak area for Benzene	Peak area for Toluene	Peak area for Xylene
10	15750	19320	22150
20	28374	36520	40817
30	43715	55428	60058
40	57362	76128	79860
50	76125	93826	108716

### A.2 Isotherm Calculation

#### A2.1 Langmuir Isotherm

Calculation of  $q_0$  in Langmuir using Equation 2.1 from the slope, and  $b$  from the intercept in Figure 4.7.

For example:

The slope for benzene in Figure 4.7.a, is 0.182,

$$\text{Slope} = 1/q_0$$

$$q_0 = 1/\text{slope} = 1/0.182 = 5.47 \text{ mg/g}$$

The intercept for benzene in Figure 4.7.a, is -0.525

$$\text{Intercept} = 1/bq_0$$

$$b = 1/q_0 (\text{Intercept}) = -0.35 \text{ L/mg}$$

## **A2.2 Freundlich Isotherm**

Calculation of  $n$  in Freundlich using Equation 2.2 from the slope, and  $K_f$  from the intercept in Fig. 4.8.

For example:

The slope for benzene in Figure 4.8.a is -0.297

$$\text{Slope} = 1/n$$

$$n = 1/\text{slope} = -3.37$$

The intercept for benzene in Figure 4.8.a, is 1.188

$$\text{Intercept} = \log K_f$$

$$K_f = 15.44 ((\text{mg/g})(\text{L/mg})^{1/n})$$

## **A.3 Kinetics Calculation**

### **A.3.1 Pseudo First Order**

The plot of  $\ln (q_e - q_t)$  versus  $t$  in Equation 2.3 for pseudo first order will give a straight line and the values of  $k_1$  and  $q_e$  (calculated) can be



obtained from the slope and the intercept of the graph 4.9 respectively.

For example:

$$\text{Slope for benzene} = -k_1 = -(-0.0123) = 0.0123 \text{ min}^{-1}$$

$$\text{Intercept} = \ln q_e = 0.409$$

$$q_e = 1.51 \text{ mg/g.}$$

### A.3.2 Pseudo Second Order

As shown in Figure 4.10, the plot of  $t/q_t$  versus  $t$  from Equation 2.4 will give  $1/q_e$  and  $1/k_2 q_e^2$  as a slope and intercept respectively.

For example:

$$\text{Slope for benzene} = 0.1174 = 1/q_e$$

$$q_e = 8.52 \text{ mg/g}$$

$$\text{Intercept} = 0.271 = 1/k_2 q_e^2$$

$$k_2 = 0.0507 \text{ g/mg.min}$$

### A.3.3 Intraparticle Diffusion Model

The  $q_t$  values are calculated by using the Equation 3.3. While, the values of  $K_i$  and  $A$  are found from the slope and the intercept of the linear plot of  $q_t$  versus  $t^{0.5}$  from Equation 2.5. The results are shown in Figure 4.11.

Example:

Calculation for benzene.

$$q_e (\text{mg} / \text{g}) = \frac{(C_0 - C_e)v}{m}$$

$$= \frac{(50 - 18) 0.05}{0.25} = 6.4 \text{ mg/g}$$

The slope =  $K_i = 0.1691 \text{ mg/g} \cdot \text{min}^{1/2}$

The intercept =  $A = 6.728$

## A.4 Thermodynamics Calculation

The thermodynamic parameters such as change in standard free energy ( $\Delta G^\circ$ ), enthalpy ( $\Delta H^\circ$ ) and entropy ( $\Delta S^\circ$ ) can be determined by using Equation 2.6, 2.7 and 2.8.

According to Equation 2.6, the  $\Delta H^\circ$ ,  $\Delta S^\circ$  parameters for BTX can be calculated from the slope and intercepts of the plot of  $\ln K_d$  versus  $1/T$  respectively (Fig. 4.12), and  $\Delta G^\circ$  values are obtained from the equation 2.8. While the values of  $K_d$  calculated by using equation 2.7.

For example

$q_e$  will be calculated using equation 3.3 as follow

$$q_e \text{ at } 15^\circ\text{C} = (50 - 7) 0.05 / 0.25 = 8.6$$

$K_d$  for benzene at  $15^\circ\text{C} = q_e / C_e = 1.229\text{L/g}$ .

$$\ln K_d = 0.21$$

$$\text{Slope} = 2997 = -\Delta H^\circ / R, R = 8.314 \text{ J/mol.K}$$

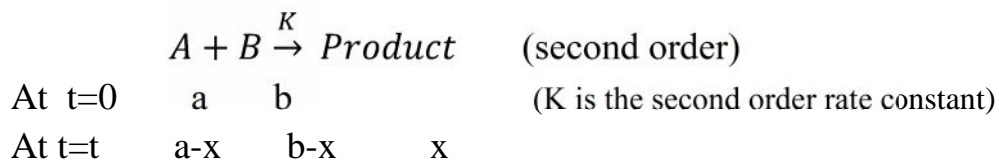
$$\Delta H^\circ = -25.16 \text{ KJ/ mol}$$

$$\text{Intercept} = -3.47 = \Delta S^\circ / R$$

$$\Delta S^\circ = -87.06 \text{ J/mol.K}$$

$$\Delta G^\circ = -RT \ln K_d = -0.50 \text{ KJ/ mol.}$$

## A.5 Pseudo-First Order Kinetics Model



$$\text{Rate} = K [A]^1 [B]^1$$

$$= K(a-x)(b-x)$$

$$\text{Rate} = -\frac{dA}{dt} = -\frac{dB}{dt}$$

$$[A] = a-x$$

$$\frac{d[A]}{dt} = \frac{d(a-x)}{dt} = \frac{da}{dt} - \frac{dx}{dt}$$

$$\frac{da}{dt} = 0$$

$$\frac{d[A]}{dt} = -\frac{dx}{dt}$$

$$\text{Rate} = -\frac{dA}{dt} = -\left(-\frac{dx}{dt}\right) = \frac{dx}{dt}$$

$$\frac{dx}{dt} = K(a-x)(b-x)$$

$$\int_0^x \frac{dx}{(a-x)(b-x)} = k \int_0^t dt \quad (\text{method of partial fraction})$$

$$t = \frac{1}{b-a} \ln \frac{a(b-x)}{b(a-x)} \quad (\text{integrated rate law for second order})$$

Because  $b \gg a, b-a \approx b, b-x \approx b$

$$Kt = \frac{1}{b} \ln \frac{ab}{b(a-x)}$$

$$Kt = \frac{1}{b} \ln \frac{a}{(a-x)}$$

$$t = \frac{1}{Kb} \ln \frac{a}{(a-x)}$$

$$Kb = K_1, a = q_e, x = q_t$$

$$t = \frac{1}{K_1} \ln \frac{q_e}{(q_e - q_t)}$$

$$\ln(q_e - q_t) = \ln q_e - k_1 t$$

## A.6 Pseudo-Second Order Kinetics Model

$$\frac{dq}{dt} = k_2(q_e - q_t)^2$$

Where,  $k_2$  is the pseudo second order rate constant of adsorption (g/mg.min),  $q_e$  is the amount of solutes sorbate sorbed at equilibrium (mg/g) and  $q_t$  is amount of solutes sorbate on the surface of the sorbent at any time  $t$  (mg/g). Separating the variables in the previous equation gives:

$$\frac{dq_t}{(q_e - q_t)^2} = k dt$$

Integrating this for the boundary conditions  $t=0$  to  $t=t$  and  $q_t=0$  to  $q_t=q_t$  gives:

$$\frac{1}{(q_e - q_t)} = \frac{1}{q_e} + kt$$

which is the integrated rate law for a pseudo-second order reaction. The equation can be rearranged to obtain:

$$\frac{t}{q_t} = \frac{1}{k_2 q_t^2} + \frac{1}{q_t} t$$

جامعة النجاح الوطنية  
كلية الدراسات العليا

## الحركية، الديناميكا الحرارية و ادمصاص مادة BTX باستخدام بذور البلح المكرينة في محلول مائي

إعداد

رشا فوزي خالد احمد

اشراف

د. شحدة جودة

د. محمد سليمان

قدمت هذه الأطروحة استكمالاً لمتطلبات الحصول على درجة الماجستير في الكيمياء بكلية الدراسات العليا في جامعة النجاح الوطنية في نابلس – فلسطين.

2014

ب

الحركية، الديناميكا الحرارية و ادمصاص مادة BTX باستخدام بذور البلح المكربنة في محلول مائي

إعداد  
رشا فوزي خالد احمد

إشراف  
د. شحدة جودة  
د. محمد سليمان

### الملخص

تعرض العالم للعديد من كوارث تلوث المياه السطحية والجوفية بمشتقات البترول في السنوات الأخيرة وخاصة تلك التي حدثت في خليج المكسيك عام ٢٠١٠. لذا كان من الضروري البحث عن وسائل التقليل من أثاره الضارة. ولتحقيق هذا الهدف تم إجراء عدة تجارب لتنقية المياه من مشتقات البترول باستخدام الكربون المنشط. ويعتبر الكربون النشط الأكثر استخداما في عملية الامتزاز نظرا لبنيته المسامية ولامتلاكه مساحة سطح كبيرة وقدرته العالية على الامتصاص.

البنزين والتلوين والزايلين هي مركبات عضوية سامة تظهر في موارد المياه الجوفية بسبب تسرب الوقود من الخزانات تحت الأرض، وكذلك التصريف غير اللائق لنفايات الصناعات النفطية والبتروكيماوية.

في هذه الدراسة تم استخدام نواة ثمرة لتحضير الكربون المنشط حيث تم غسلها بالماء للتخلص من الشوائب ثم جففت على درجة ١١٠ درجة مئوية لمدة ٢٤ ساعة وسحقت ثم مزجت مع محلول  $FeCl_3$  أو  $CuSO_4 \cdot 5H_2O$  أو  $AgNO_3$  كمادة منشطة بنسبة تشريب ١:٢ لمدة ٢٤ ساعة على درجة حرارة الغرفة. وقد جففت العينات المشربة بالمادة المنشطة على درجة حرارة ١١٠ مئوية، ثم استخدام جهاز Tube Furnace من اجل كربنة العينات وذلك على درجة حرارة تنشيط تصل إلى ٧٠٠ درجة مئوية.

ت

وأشارت النتائج في هذا العمل إلى أن الكربون المنشط باستخدام  $FeCl_3$  هو الأفضل في امتزاز البنزين والتلوين والزايلين. وقد تم دراسة اثر الوقت ودرجة الحرارة ودرجة الحموضة وكمية الكربون المستخدم على قدرة الكربون على الامتزاز. وتشير النتائج إلى أن فعالية الامتزاز زادت بزيادة درجة الحموضة وكمية الكربون والوقت، بينما قلت الفعالية بزيادة درجة الحرارة.

وفسرت نتائج الامتزاز التي تم الحصول عليها عند الاتزان باستخدام معادلتى فريندليش و لانجموير، وقد استطاع نموذج لانجموير تفسير عملية الامتزاز.

ولمعرفة آلية الامتزاز، أجريت دراسة على ثلاثة أنظمة للحركة هي: نظام الاعتماد من الدرجة الأولى ظاهريا ونظام الاعتماد من الدرجة الثانية ظاهريا ونظام تدفق الدقائق إلى داخل الجسيمات. وقد وجد أن الامتزاز يتبع نظام الاعتماد من الدرجة الثانية.

تم أيضا حساب ثوابت الديناميكا الحرارية وهي طاقة غيبس  $\Delta G^\circ$  والمحتوى الحراري  $\Delta H^\circ$  والتغير في الفوضى  $\Delta S^\circ$ . أما شكل وحجم مساحة السطح للعينات فقد تم تحديدها باستخدام طريقة Iodine Number و BET وجهاز SEM.